Pedestrian Impact Analysis Considering U.S. Vehicle Fleet: Crash Reconstruction and Validation Study using VICIS Database

Jaehyuk Heo, Joon Seok Kong, Katarzyna Rawska, Jason R. Kerrigan, Taewung Kim, Bronislaw D. Gepner

Abstract In this study, we aim to reconstruct three real-world pedestrian crashes informed by VICIS database and check the applicability of current pedestrian protection regulations to the U.S. vehicle fleet. Three cases were selected to represent large SUVs and trucks, small SUVs, and sedans. FE vehicle models were validated through Euro NCAP-style impactor tests and used to simulate detailed pedestrian-vehicle crash scenarios with a 50th percentile male THUMS human body model. The reconstruction results showed good agreement with observed vehicle deformations and injury outcomes. This study also found that Euro NCAP-style upper and lower legform impactor responses corresponded well with femur and lower extremity injuries observed in reconstruction simulations. Kinematic differences were observed across vehicle types, with the SUV and truck cases showing earlier and more direct thoracic engagement compared to the sedan case due to their elevated front-end geometries. This region, which remains untested in current protocols, was associated with high rib strain, particularly in the lower ribs of the 50th male pedestrian. These findings highlight the limitations of existing test procedures and underscore the need for expanded pedestrian safety assessment methods for modern U.S. vehicles.

Keywords crash reconstruction, pedestrian safety, Euro NCAP pedestrian protection protocol, thorax injury, front-end geometry

I. INTRODUCTION

In the United States (U.S.), pedestrian fatalities are on the rise [1-4]. Between 2000 and 2020, pedestrian fatalities increased by 37%, while occupant fatalities decreased from 32,225 in 2000 to 23,824 in 2020, indicating progress in occupant protection [4]. In comparison, other developed nations, such as the European Union (EU) and Japan, experienced either decrease or no change in pedestrian fatalities. Various factors, including infrastructure and driver behavior, may have contributed to different pedestrian safety trends. However, one other thing that distinguishes U.S. from the other parts of the world is the lack of safety regulations focusing on pedestrian safety. From the perspective of crashworthiness ratings, pedestrian testing requirements using headforms and legforms appear to be effective in influencing vehicle manufactures to innovate vehicle designs and adopt active safety technologies, considering U.S., European and Japanese variants of the same vehicle models [29-30].

In [4], the National Highway Traffic Safety Administration (NHTSA) announced an intention for pedestrian protection evaluation into the updated New Car Assessment Program (NCAP). The proposed testing methodology aligns with the European NCAP (Euro NCAP), which was derived from Global Technical Regulation No. 9 (GTR No.9) [5-6]. The proposed evaluations assess the risk of head, pelvis, leg, and knee injuries to pedestrians in collisions with the front of vehicles. However, the test procedures and requirements in GTR No.9 were originally developed for sedan-type passenger cars [7-8]. Although these tests are useful for improving the safety of pedestrians, it is noted in GTR No. 9 that not all vehicles comply with these technical provisions. Therefore, the applicability of the Euro NCAP test protocol to the U.S. vehicle fleet may not be feasible, particularly given that Sport Utility Vehicles (SUVs) and trucks now dominate the U.S. market, accounting for 75% sales in the U.S. [9-10].

Field data studies consistently indicate that larger vehicles, such as SUVs and trucks, are more likely to cause injuries to pedestrians compared to sedans. In [11], the authors conducted a meta-analysis of 12 studies, showing that the risk of fatal injury to pedestrians is 50% greater in collisions with light trucks than with passenger cars. In [12], the authors reported that SUVs and pickup trucks were more likely to kill pedestrians and pedal cyclists. The

J. Heo is a Research Specialist (+1-434-320-9428 / zud7hh@virginia.edu), J. S. Kong was a Postdoctoral Research Associate, K. Rawska is a Laboratory Specialist Senior, J. R. Kerrigan is a Commonwealth Professor of Mechanical and Aerospace Engineering at University of Virginia, USA., T. Kim is an Associate Professor of Mechanical Design Engineering at Tech University of Korea, B. D. Gepner is a Senior Scientist.

study also found that children were eight times more likely to die when struck by an SUV compared to a passenger car. Reference [13] further highlighted a shift in pedestrian injury patterns over time, with an increasing rate of thorax and pelvis injuries, likely due to the increasing proportion of SUVs and trucks in the U.S. vehicle fleet. In [14], the authors supported these concerns by showing that SUVs are 2-3 times more likely to cause fatal pedestrian injuries than smaller passenger cars, due to the greater likelihood of direct torso impacts.

The geometry of SUVs and trucks differs from that of sedans, leading to unique pedestrian kinematics and injury mechanisms. In [15], the authors found that vehicles with Hood Leading Edge (HLE) heights above a pedestrian's waist resulted in a higher risk of AIS 2+ torso injuries due to direct impacts with vehicle front-end. Similarly, reference [16] reported that a high HLE combined with a blunt front-end increased the severity of pedestrian injuries in the torso and hip regions. Reference [17] further supported these findings, emphasizing that pedestrians struck by taller vehicles experience different injury mechanisms than those struck by sedans. Given these differences, the existing testing framework does not fully represent pedestrian-vehicle interactions, as it can fail to evaluate critical impact areas specific to taller vehicles. Consequently, existing pedestrian safety evaluation methods, such as headform, upper legform, and lower legform tests, may need to be revised or supplemented to better reflect real-world crash scenarios. Therefore, it is important to assess the effectiveness of current pedestrian protection standards with respect to vehicle front end geometry.

Simulation studies are essential for providing valuable reference into the development of improved testing protocols, as they allow for exploring various crash scenarios, material properties, and even the potential benefits of countermeasures. For this reason, recent studies have conducted pedestrian-focused studies through the reconstruction of real-world crashes. In [18], the authors reconstructed 25 pedestrian crash cases to better understand the new trends in pedestrian injuries and explored the potential effectiveness of Pedestrian Automatic Emergency Braking (PedAEB) in reducing injury risk. However, this study utilized simplified multi-body simulations, which may not fully capture the complex interactions between pedestrians and different vehicle types. In [19], the authors addressed this limitation by employing a hybrid simulation approach, using multibody simulations to reconstruct crash scenarios and Finite Element (FE) simulations with the Total human Model for Safety (THUMS) model for detailed injury analysis. Their study showed good agreement between simulation and observed injuries, especially in the lower limbs, but relied on simplified, rigid vehicle models that lacked structural deformation. As a result, the interaction between the pedestrian and deformable front-end components, which may play a critical role in injury mechanisms, may not have been fully represented. This highlights the need for fully deformable vehicle models to improve the fidelity of pedestrian crash reconstruction and injury prediction, particularly when evaluating modern U.S. vehicles such as sedans, SUVs, and trucks, in order to investigate the applicability of existing pedestrian protection regulations.

The goal of this study is to evaluate the suitability of fully deformable FE vehicle models originally validated in frontal crash scenarios for pedestrian crash analysis, as a foundation for developing improved impactor-based test protocols and future large-scale parametric studies. These studies would consider the variability in front-end geometry and material properties across representative U.S. vehicle types, including sedans, SUVs, and trucks. Real-world crash scenarios were selected based on a thorough review of Vulnerable road user In-depth Crash Investigation Study (VICIS) database. By integrating real-world crash data with virtual simulations, this research reconstructed specific cases to examine how vehicle type influences pedestrian injury risk and assessed whether FE vehicle models can effectively represent pedestrian crashes. Furthermore, this study aims to address the question of applicability of the established pedestrian crashworthiness standards to the current U.S. vehicle fleet.

II. METHODS

The steps are as follows. First, three VICIS cases were selected based on several criteria, including representation of the current U.S. vehicle fleet, pedestrian anthropometry, and data availability. Second, three FE vehicle models representing different sizes within the U.S. vehicle fleet were developed. To reduce computational load, the models were modified by removing vehicle parts that do not contribute to pedestrian-vehicle interactions. Third, component-level validation was conducted using established pedestrian protection protocols. This step involved Euro NCAP-style impactor tests across multiple locations on each vehicle model. Fourth, the information obtained from the three VICIS cases was incorporated into the FE models to perform simulation-based reconstructions. The pedestrian was represented using THUMS AM50 V4.02. All simulations in this study were carried out using LS-DYNA FE solver. Lastly, the injury outcomes were analyzed to assess how well the simulation results reflected real-world crash outcomes. Fig. 1 shows an overview of the methodology.

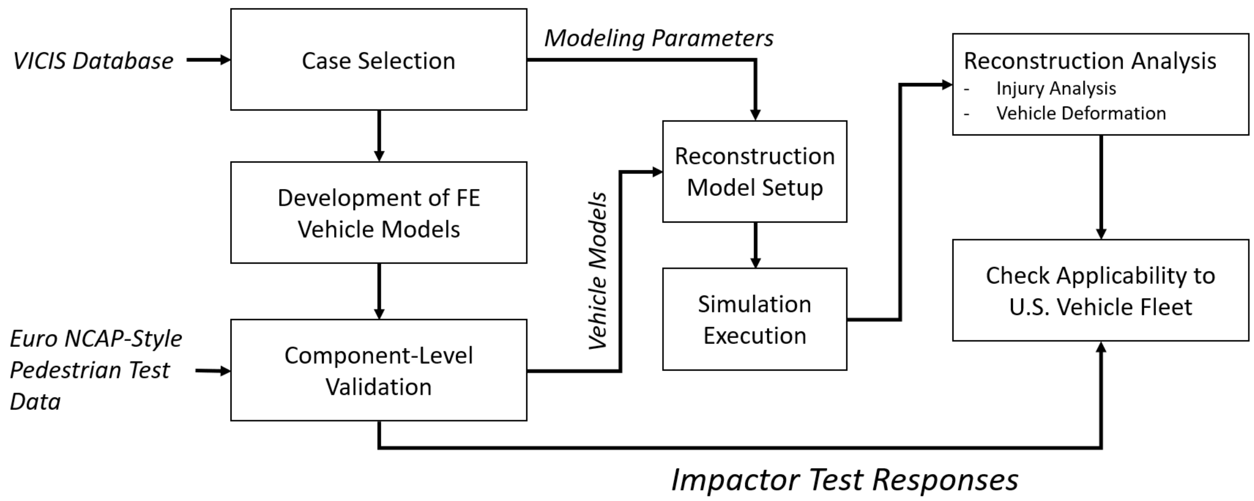

Fig. 1. Overview of the pedestrian crash reconstruction and evaluation method.

VICIS Case Selection

NHTSA has made VICIS database publicly available, focusing on pedestrian crash cases involving impacts to the frontal plane of passenger vehicles manufactured in 2004 or later. The case review and analysis process for VICIS followed the same methodology as the Crash Injury Research and Engineering Network (CIREN), with necessary modifications [43]. Several key criteria were considered in selecting specific VICIS cases for pedestrian reconstruction. First, vehicle type was considered to ensure that the selected cases represent the current U.S. vehicle fleet, including large SUVs and trucks, small SUVs, and sedans. Second, the crash conditions must be described with sufficient detail to allow for accurate reconstruction in simulation. Third, the availability of detailed open-source FE vehicle models that could effectively represent the U.S. vehicle fleet was considered to ensure compatibility and high simulation quality. Fourth, the availability of component test data for each vehicle type was considered to support the reliability of the FE model responses. Lastly, pedestrian anthropometry was considered, with this study focusing on a 50th percentile male pedestrian. Based on these criteria, three VICIS cases were selected with detailed information provided in Table I and Table IV.

Pedestrian-Focused FE Vehicle Model Development

To represent different vehicle categories within the U.S. fleet, three detailed open-source FE vehicle models were selected [20]: 2014 Chevrolet Silverado, 2020 Nissan Rogue, and 2015 Toyota Camry. Each model represents a distinct vehicle type, with the Silverado representing large SUVs and trucks, the Rogue representing small SUVs, and the Camry representing sedan-like passenger cars. These vehicle models were modified from detailed FE models. Non-interactive vehicle parts, such as internal seat configurations and tires were removed. Additionally, the rear end of each vehicle was rigidized to make it easier to apply boundary conditions. These modifications were intended to reduce computational load while maintaining pedestrian-relevant impact zones, particularly bumper, grille, headlights, and hood areas, which are known to cause AIS 3+ injuries [14].

Component-Level Validation of FE Vehicle Models

To ensure the reliability of the model responses in pedestrian impact scenarios, component-level validation was performed using Euro NCAP test procedures and recent experimental data. Publicly available test results were used as reference data. In 2019, NHTSA carried out a study focusing on the current state of pedestrian protection in the U.S. vehicle fleet [21]. The study utilized the pedestrian test procedures established by Euro NCAP, which involved headform impacts to the hood and windshield, as well as impacts using upper and lower legforms to the vehicle front end. A total of nine vehicles were tested, including passenger cars, a minivan, SUVs, and pickup trucks.

Four tested vehicles were identified as reasonable candidates for comparison, although none of them precisely matched the simulation models. One of the tested vehicles was the 2016 Chevrolet Tahoe, which shares its vehicle platform with 2014 Chevrolet Silverado used in the FE simulations. The 2014 Chevrolet Silverado model also reveals geometric similarities with the 2016 Chevrolet Tahoe. For example, the overall dimensions are 80 in (width) × 73.8 in (height) for the 2014 Silverado and 80.5 in (width) × 74.4 in (height) for the 2016 Tahoe. Similarly, the 2016 Nissan Rogue was also tested in the NHTSA study. While Rogue went through a facelift in 2017, it was a minor model year change, which included cosmetic changes to the headlights and the grille, meaning that the results from the 2016 model should be applicable to the 2020 model used in the FE simulations. For sedans, the NHTSA study tested 2017 Audi A4 and 2016 Chevrolet Malibu. Although these models differ dimensionally from 2015 Toyota Camry simulation model, they still represent key characteristics of sedan-type vehicles. Given that vehicle shape significantly influences the interaction between impactors and the front-end, these sedans were considered appropriate for component validation to check whether the simulation model reasonably captures vehicle stiffness and shape effects. Consequently, the tested vehicles listed in Table I were selected for comparison with the simulation models. Simulation models were first validated using NHTSA test data. After validation, they were then used to reconstruct the corresponding VICIS cases.

TABLE I

SUMMARY OF TESTED VEHICLES, SIMULATION MODELS FOR COMPONENT VALIDATION, AND CORRESPONDING VICIS CASES IN CRASH RECONSTRUCTION

Vehicle Type	NHTSA Test Data	Simulation Model	VICIS Cases
Large SUVs and Trucks	2016 Chevrolet Tahoe	2014 Chevrolet Silverado	2016 Chevrolet Silverado
Small SUVs	2016 Nissan Rogue	2020 Nissan Rogue	2020 Nissan Rogue
Sedans	2017 Aido A4 & 2016 Chevrolet Malibu	2015 Toyota Camry	2020 Toyota Camry

Based on Euro NCAP pedestrian testing protocol used in [21], grid points corresponding to impact locations were calculated on each FE vehicle model to ensure consistency with experimental test conditions. For upper legform impacts, grid points were marked along the Wrap Around Distance (WAD) of 775 mm in 100 mm lateral increments from the vehicle centerline. For headform impact tests, grid points were labeled starting at WAD 1000 and extended rearward in 100 mm increments, with 100 mm lateral increments. Additionally, the lower legform impactor was positioned 75 mm above the ground and aligned laterally in 100 mm increments from the vehicle centerline. For the Toyota Camry simulation model, headform impact locations were shifted forward by 100 mm due to its shorter hood compared to the Audi A4 and Chevrolet Malibu. For example, the (8,0) grid point used in the tests was adjusted to (7,0) in the simulation. Fig. 2 shows the grid points assigned based on the WRD. All grid points were projected onto the nearest continuous surface of the hood or bumper of each vehicle, excluding any gaps or discontinuities such as the space between the bumper and grille, to determine their coordinates. Red dots represent the locations along the vehicle centerline, while blue dots were symmetrically calculated based on the red dots. The velocity and angle conditions for the headform and upper legform, as well as the velocity condition for the lower legform, were all applied to match those used in the corresponding experimental tests.

After completing the simulations, the results were qualitatively compared with experimental test data, including acceleration, force, and moment signals. For quantitative evaluation, the correlation between time-history signals from the tests and simulations was assessed using the objective rating metric defined in ISO/TS 18571 [31]. In the headform tests, each case involved a single acceleration signal, so the rating was calculated by directly comparing the test and simulation signals. In contrast, the upper legform and lower legform tests involved multiple signals. The upper legform test included six signals, such as impactor velocity, femur forces, and femur moments. Similarly, the lower legform test used six signals, including knee displacements and tibia moments. In these cases, a rating was computed for each individual signal, and the average of these rating was used to represent the corresponding test. For the Camry case, two test vehicles were used. Some signals were available from both vehicles, while others were available from only one due to limited data. When data from both vehicles were available, the ratings were calculated separately for each vehicle and then averaged to obtain a representative value. The correlation scores were classified as follows: Excellent (rating $>$ 0.94), Good (0.94 $\geq$ rating $>$ 0.8), Fair (0.8 $\geq$ rating $>$ 0.58), and Poor (0.58 $\geq$ rating).

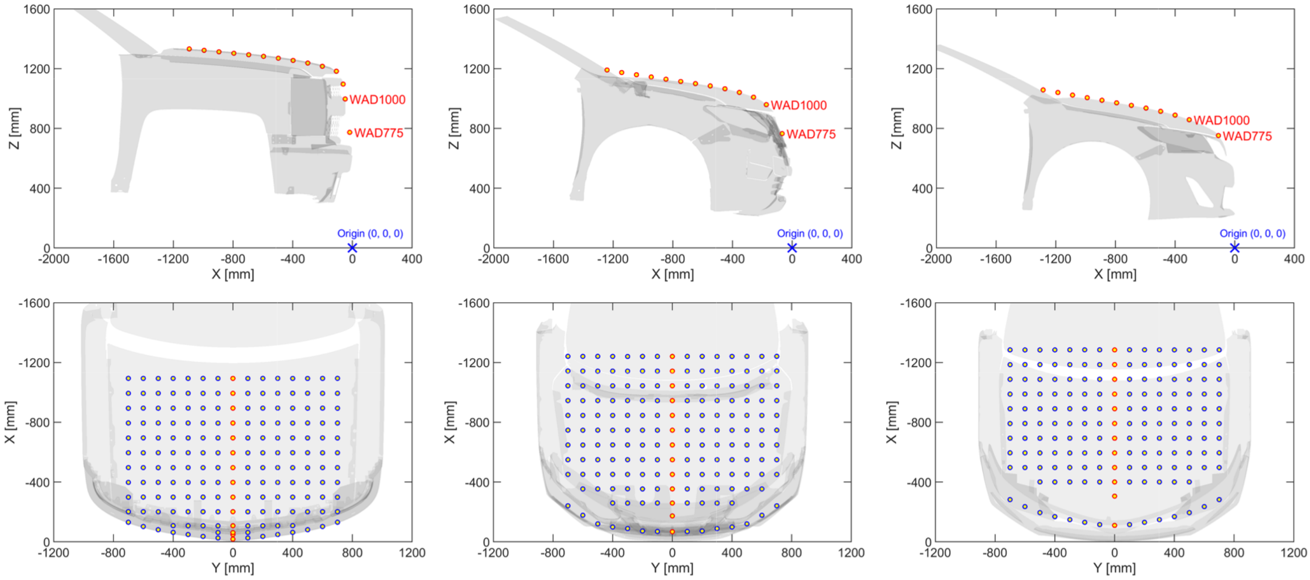

Fig. 2. Grid points for impact locations on FE vehicle models based on the Euro NCAP protocol (top: side view; bottom: top view). From left to right: Chevrolet Silverado, Nissan Rogue and Toyota Camry.

Crash Reconstruction Based on the VICIS Database

Three FE vehicle models were used to reconstruct selected VICIS cases. Each reconstruction incorporated crash parameters, including vehicle impact speed, pedestrian-vehicle contact points (e.g., bumper, hood, windshield). If the vehicle impact speed was unknown, the speed limit of the road where the crash occurred was used as the vehicle impact speed. Due to the lack of detailed information, we assumed a pure lateral impact, no pedestrian movement, and no vehicle braking for the reconstruction cases. Additionally, THUMS AM50 V4.02 model for TB024 scenario, which includes a pre-defined pedestrian posture (left leg forward, right leg backward; impact leg depending on pedestrian orientation), was applied. THUMS AM50 was employed for all cases without any anthropometric scaling procedures. The results from the reconstructed simulations were then compared with actual injury data from VICIS cases.

An internally developed injury prediction suite was utilized to check that THUMS could effectively capture real-world pedestrian injuries. The injury prediction suite was originally developed for assessing occupant injuries in frontal crashes and the suite can predict over 100 injury metrics across all body regions. For the pedestrian crash cases, the suite was applied without modification, so there remains room for improvement to better capture pedestrian-specific injury predictions. Table II shows the injury metrics used as criteria, which correspond to the results shown in Table IV and Table V. To compare the overall prediction accuracy across different vehicles, confusion matrix was used to classify each injury outcome into true positive (TP), true negative (TN), false positive (FP), and false negative (FN) [42]. Then, the accuracy was calculated for each vehicle type.

TABLE II

INJURY METRICS FOR INJURY RISK PREDICTION

Body Region	Injury Metric (or Predictor)	Predicted Injury Type	Predicted AIS Level
Head	HIC15	Skull Fracture [32]	AIS 2+, AIS 3+
Cervical Spine	Nij	Fractures of Individual Cervical Vertebrae [33]	AIS 2+, AIS 3+
Thorax	Rib Strain	3+ Rib Fractures [34]	AIS 3+
Lumbar Spine	Lfx	Fractures of Individual Lumbar Vertebrae [35]	AIS 3+
Arm	A-P Bending Moment	Humerus Fracture [36]	AIS 2+
Forearm	A-P Bending Moment	Forearm Fracture [37]	AIS 2+
Pelvis	Lateral Deflection	Pelvis Fracture [38]	AIS 2+
Thigh	L-M Bending Moment (Femur)	Femur Fracture [39]	AIS 3+
Knee	Lateral Bending Angle	Knee Ligament Rupture [40]	AIS 2+
Leg	L-M Bending Moment (Tibia)	Tibia Fracture [39]	AIS 2+
Foot	Axial Force (Tibia)	Calcaneus, Talus, Ankle, and Midfoot Fractures [41]	AIS 2+

III. RESULTS

Developed FE Vehicle Models for Pedestrian Studies

In all three models, the rear of the vehicle structures, seats, seat mounting components, tires, and other non-essential parts were eliminated. To facilitate prescribed motion, the rear end of each vehicle was converted into the rigid part (shown in yellow). To accurately reflect the relative height between the pedestrian and the vehicle, the ground plane was positioned at the tire contact points. As shown in Fig. 3, the three simulation models exhibit distinct vehicle sizes, front-end shapes, and HLE heights. As a result, an optimized set of FE vehicle models, representing trucks, SUVs, and sedans, was successfully developed.

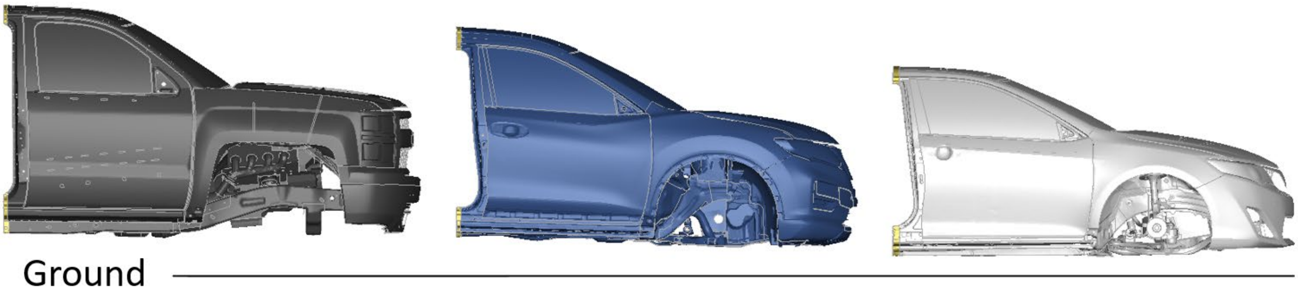

Fig. 3. FE vehicle models developed for pedestrian-vehicle interaction. The models were developed based on detailed open-source FE models. From left to right: Chevrolet Silverado (black), Nissan Rogue (blue) and Toyota Camry (white), representing trucks, SUVs, and sedans, respectively. The rigid rear part of each vehicle (shown in yellow) was intended to facilitate prescribed motion.

Comparison of Test and Simulation Data: Component-Level Validation

Table III and Appendix A present the results of component-level validation by comparing headform, upper legform, and lower legform impactor test outcomes between experimental tests and simulations for three vehicles: Chevrolet Silverado, Nissan Rogue, and Toyota Camry. The evaluation was based on response signals such as acceleration, displacement, force, and moment. The results indicated that the Tahoe and Silverado models exhibited reasonable correlation under headform and lower legform impact conditions, with similar peak values and durations in the relevant signals. In contrast, some discrepancies were observed in the upper legform tests, although certain signals still showed acceptable similarities. A similar trend was observed for the Rogue, which demonstrated fair agreement in headform and lower legform results but exhibited notable discrepancies in the upper legform responses. The Camry model, on the other hand, showed relatively lower correlation overall compared to the other vehicles (A4 and Malibu), potentially due to differences in hood dimensions and front-end structure.

Quantitative evaluation using ISO/TS 18571 revealed average ratings for the headform tests of 0.73, 0.70, and 0.62 for the Silverado, Rogue, and Camry, respectively. These values indicate fair agreement. While the models did not match the test vehicles exactly, the results could be considered acceptable, as they show a reasonable response in terms of headform impacts. In contrast, the upper legform tests produced lower scores, with average ratings of 0.51, 0.56, and 0.50 for the Silverado, Rogue, and Camry, respectively. These ratings are classified as poor agreement. These results reflect limitations in accurately simulating the upper legform impacts. For the lower legform tests, the Silverado (0.74) and Rogue (0.64) achieved fair agreement, while the Camry scored 0.47, which fell into the poor category. Although the Camry exhibited lower correlation, a similar trend was observed in the other tested sedan-type vehicles, suggesting that two tested vehicles showed quite different signals, likely due to differences in the vehicle models. Since the Camry also differs from other test models (A4 and Malibu), this result may still be considered reasonable. Overall, these findings suggest that while headform and lower legform components achieved reasonable agreement with experimental data, especially when considering the differences in vehicle models, upper legform validation remains a significant challenge across all vehicle models.

TABLE III

OBJECTIVE RATING RESULTS FOR THREE FE VEHICLE MODELS

Test Type	Chevrolet Silverado			Nissan Rogue			Toyota Camry		
	Test ID	Rating	Grade	Test ID	Rating	Grade	Test ID	Rating	Grade
Headform	A1635	0.67	Fair	A1601	0.7	Fair	A,7,0	0.53	Poor
	A1636	0.7	Fair	A1602	0.81	Good	A,7,5	0.48	Poor
	A1637	0.79	Fair	A1603	0.74	Fair	A,8,-7	0.56	Poor
	A1638	0.71	Fair	A1604	0.81	Good	C,0,0	0.82	Good
	A1642	0.79	Fair	C1605	0.77	Fair	C,1,-5	0.68	Fair
	C1632	0.62	Fair	C1606	0.74	Fair	C,2,0	0.34	Poor
	C1633	0.55	Poor	C1607	0.74	Fair	C,2,6	0.6	Fair
	C1634	0.76	Fair	C1608	0.52	Poor	C,2,-7	0.72	Fair
	C1639	0.7	Fair	C1609	0.8	Fair	C,3,2	0.73	Fair
	C1640	0.83	Good	C1610	0.54	Poor	C,6,0	0.64	Fair
	C1641	0.87	Good	C1611	0.5	Poor	C,6,5	0.77	Fair
							C,6,-6	0.71	Fair
							C,4,5	0.55	Poor
							A,10,0	0.55	Poor
	Average : 0.73 (Fair)			Average : 0.7 (Fair)			Average : 0.62 (Fair)		
Upper Legform	UL1651	0.59	Fair	UL1610	0.42	Poor	U+1	0.54	Poor
	UL1652	0.44	Poor	UL1611	0.72	Fair	U-3	0.47	Poor
	UL1653	0.6	Fair	UL1612	0.6	Fair	U+5	0.61	Fair
	UL1654	0.39	Poor	UL1613	0.48	Poor	U-7	0.37	Poor
	Average : 0.51 (Poor)			Average : 0.56 (Poor)			Average : 0.5 (Poor)		
Lower Legform	LL1616	0.76	Fair	LL1605	0.57	Poor	L+1	0.47	Poor
	LL1617	0.7	Fair	LL1606	0.66	Fair	L+5	0.38	Poor
	LL1618	0.75	Fair	LL1611	0.68	Fair	L-3	0.41	Poor
							L-7	0.62	Fair
	Average : 0.74 (Fair)			Average : 0.64 (Fair)			Average : 0.47 (Poor)		

Summary of Selected VICIS Cases

Table IV provides a summary of the VICIS cases selected for pedestrian crash reconstruction. Each case includes key details about the pedestrian, vehicle, and event conditions. All cases involved male pedestrians, aged 54 to 65 years, with heights ranging from 170 cm to 183 cm and weights between 73 kg and 79 kg. The Injury Severity Score (ISS) varied from 43 to 75, and the Maximum Abbreviated Injury Scale (MAIS) ranged from 5 (Critical) to 6 (Maximal). The selected crashes involved three different vehicle types: 2020 Toyota Camry (representing sedans), 2020 Nissan Rogue (representing small SUVs), 2016 Chevrolet Silverado (representing large SUVs/trucks). The speed limit at the crash locations ranged from 64 km/h (40 mph) to 97 km/h (60 mph). Actual vehicle impact speeds varied from 60 km/h to 89 km/h, with the Silverado case having an unknown impact speed. The number of AIS-reported injuries varied across cases, with 56, 42, and 37 injuries reported for the Camry, Rogue, and Silverado cases, respectively. The numbers (e.g., 56 reported) refer to the total number of injuries reported.

TABLE IV
VICIS SUMMARY

Case	ID	1024	1141	1226
Case Non-Motorist	Sex	Male	Male	Male
	Age (years)	54	65	55
	Height (cm)	170	178	183
	Weight (kg)	73	78	79
	ISS	45	75	43
	MAIS	5 - Critical	6 - Maximal	5 - Critical
Case Vehicle	Model Year	2020	2020	2016
	Make	Toyota	Nissan	Chevrolet
	Model	Camry	Rogue	Silverado
Event Details	Speed Limit (mph)	40	60	45
	Vehicle Speed (mph)	37	55	Unknown
	Impact Side of Pedestrian	Left side	Anterior or right side	Left side
Injury Summary	AIS Description	56 reported	42 reported	37 reported

VICIS Reconstruction – Model Setup

Fig. 4 shows the final model setup along with the observed contact areas, components, and Y-offset values derived from each VICIS case. All impacts were assumed to be pure lateral impact, without considering detailed pedestrian orientation. Specifically, the Silverado case involved a left-side impact to the pedestrian, the Rogue involved a right-side impact, and the Camry involved a left-side impact. The number of contact points provided varied by case (five for the Silverado, three for the Rogue, and four for the Camry). Each contact point was referenced relative to the vehicle's centerline. The pedestrian model was laterally offset based on the average Y-position of all contact points for each case. Vehicle impact speeds were applied based on case records; however, for the Silverado case, where the actual speed was unknown, the speed limit was used instead.

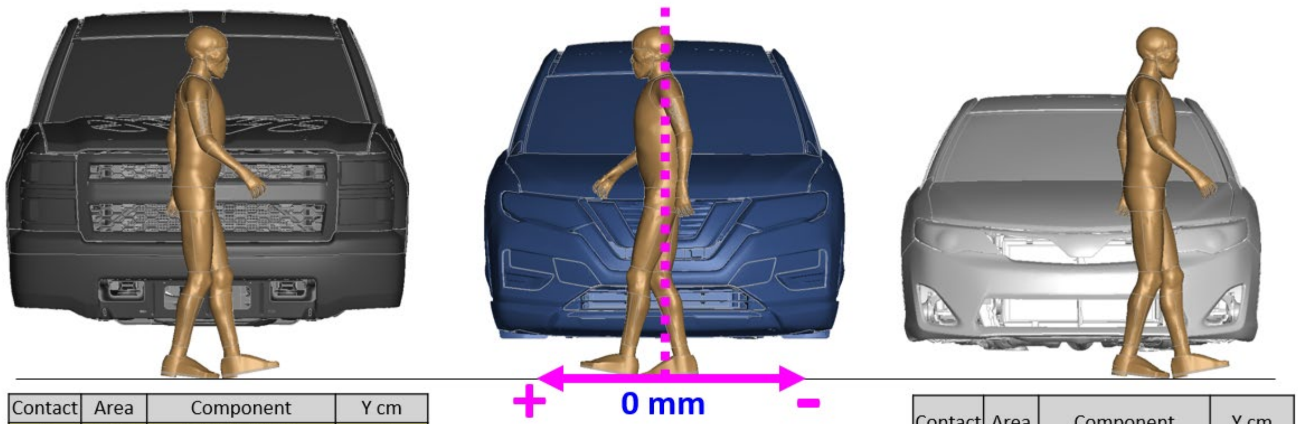

Contact	Area	Component	Y cm
A	Front	Front bumper	-4
B	Front	Front grille	5
C	Top	Hood surface	5
D	Top	Hood surface	-12
E	Front	Hood edge and/or trim	7

Contact	Area	Component	Y cm
A	Top	Hood surface	4
C	Front	Front lower valance/spoiler	-5
D	Front	Front grille	20

Contact	Area	Component	Y cm
A	Front	Front lower valance/spoiler	-32
C	Front	Front grille	-33
D	Front	Hood edge and/or trim	-44
E	Top	Hood surface	-47

Fig. 4. Final simulation setup with pedestrian lateral offset based on VICIS contact point data.

VICIS Reconstruction – Pedestrian Kinematics

Figures 5, 6, and 7 shows pedestrian kinematics for the Silverado, Rogue, and Camry cases, respectively. Due to the different impact speeds applied in each case, direct kinematic comparisons at the same time are not possible. In the Silverado case, the lower extremities and thorax initially contact the vehicle, followed by the pelvis, which moves along with deformation of the grille. In contrast, the knee and thorax experience concentrated loading due to minimal deformation in the bumper and HLE. The head ultimately impacts the hood, not the windshield. In the Rogue case, the lower extremities and pelvis make initial contact. As the bumper and hood deform, wrap-around kinematics are observed, leading to head impact on the windshield. For the Camry case, the lower extremities contact the vehicle first, followed by the pelvis during the wrap-around motion along the front end. The upper body swings downward over the hood, and the head impacts the windshield.

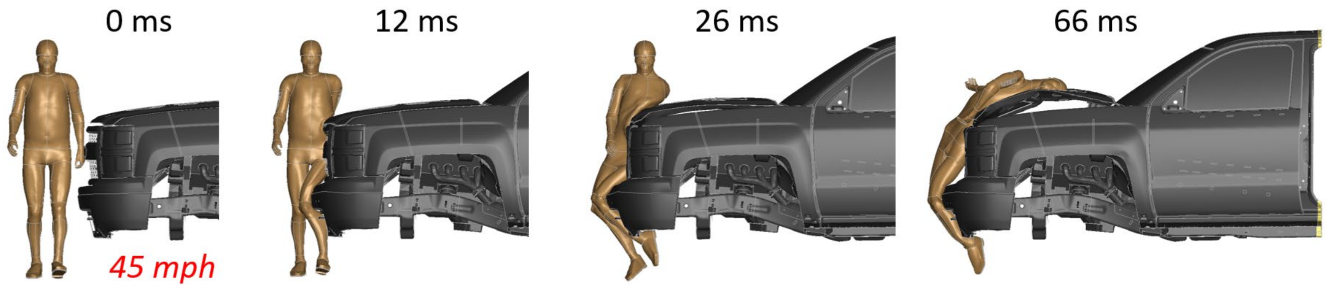

Fig. 5. Pedestrian kinematics for Silverado case (45 mph).

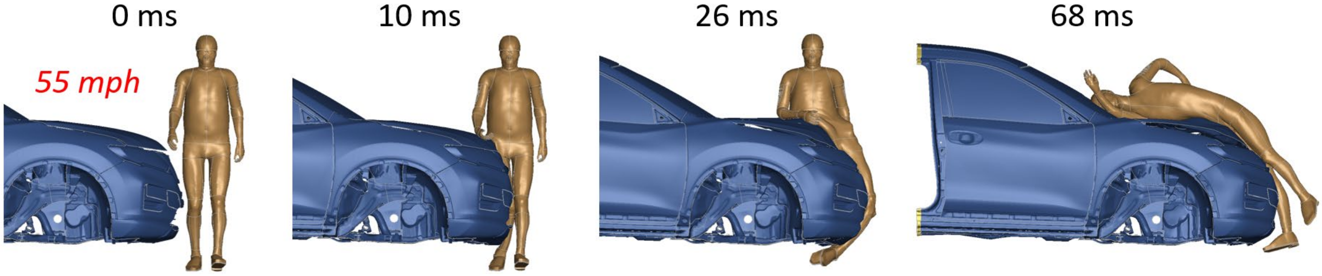

Fig. 6. Pedestrian kinematics for Rogue case (55 mph).

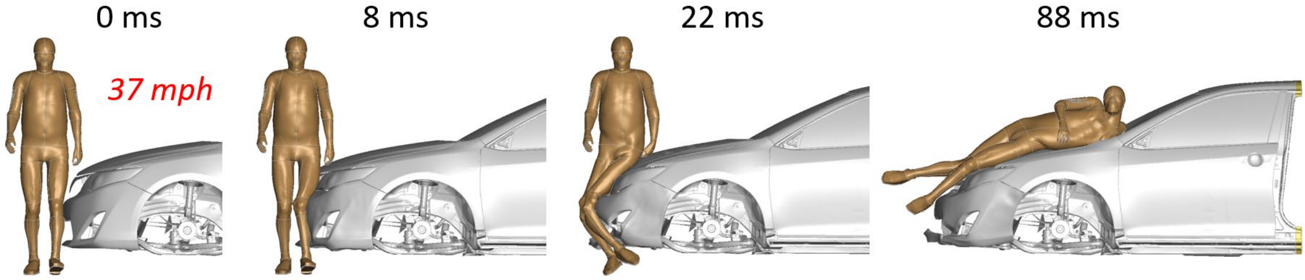

Fig. 7. Pedestrian kinematics for Camry case (37 mph).

VICIS Reconstruction – Injury Analysis

The VICIS report provides highly detailed injury descriptions, including medical terminology and classification. The report includes both AIS Descriptions and AIS Severity levels. The AIS Description includes not only the injured body region but also the potential injury mechanism. Multiple AIS descriptions may exist for the same injury location, due to variations in medical classification. However, current Human Body Models (HBMs) have limitations in capturing detailed injury mechanisms within the same body region. Given these constraints, the analysis focused on comparing MAIS for each body region. Injuries were categorized as AIS 2+ or AIS 3+. As shown in Table V, each body region was labeled as 1 if the MAIS was AIS 2 or higher, and 0 otherwise. Similarly, THUMS-predicted probabilities of AIS 2+ injuries were binarized: values of 0.5 or greater were labeled as 1, and values below 0.5 were labeled as 0. This process was applied consistently across all three vehicles. The same procedure was also applied for AIS 3+ injuries, as shown in Table VI.

TABLE V
COMPARISON OF OBSERVED AND PREDICTED AIS 2+ INJURIES BY BODY REGION

Body Region	Chevrolet Silverado			Nissan Rogue			Toyota Camry		
	AIS 2+ (Observed)	Prob. of AIS 2+ (Predicted)	Confusion Matrix	AIS 2+ (Observed)	Prob. of AIS 2+ (Predicted)	Confusion Matrix	AIS 2+ (Observed)	Prob. of AIS 2+ (Predicted)	Confusion Matrix
Head	1	0.825 (1)	TP	1	0.999 (1)	TP	1	0.985 (1)	TP
Cervical Spine	1	0.968 (1)	TP	1	0.825 (1)	TP	1	0.949 (1)	TP
Thorax	1	N/A	---	1	N/A	---	1	N/A	---
Lumbar/ Thoracic Spine	0	N/A	---	1	N/A	---	0	N/A	---
Shoulder	1	N/A	---	1	N/A	---	0	N/A	---
Arm	0	0.02 (0)	TN	1	0.012 (0)	FN	0	0.01 (0)	TN
Forearm	0	0.09 (0)	TN	0	0.226 (0)	TN	0	0.054 (0)	TN
Pelvis	0	0.319 (0)	TN	1	0.999 (1)	TP	1	0.831 (1)	TP
Thigh	1	N/A	---	1	N/A	---	0	N/A	---
Knee	1	0.999 (1)	TP	0	0.999 (1)	FP	0	0.999 (1)	FP
Leg	1	0.584 (1)	TP	0	0.108 (0)	TN	0	0.115 (0)	TN
Ankle	0	N/A	---	0	N/A	---	0	N/A	---
Foot	0	0.199 (0)	TN	0	0.106 (0)	TN	0	0.077 (0)	TN
		Accuracy : 100%			Accuracy : 75%			Accuracy : 87.5%	

TABLE VI
COMPARISON OF OBSERVED AND PREDICTED AIS 3+ INJURIES BY BODY REGION

Body Region	Chevrolet Silverado			Nissan Rogue			Toyota Camry		
	AIS 3+ (Observed)	Prob. of AIS 3+ (Predicted)	Confusion Matrix	AIS 3+ (Observed)	Prob. of AIS 3+ (Predicted)	Confusion Matrix	AIS 3+ (Observed)	Prob. of AIS 3+ (Predicted)	Confusion Matrix
Head/Face	1	0.659 (1)	TP	1	0.997 (1)	TP	1	0.966 (1)	TP
Cervical Spine	1	0.877 (1)	TP	1	0.7 (1)	TP	1	0.844 (1)	TP
Thorax	1	0.999 (1)	TP	1	0.999 (1)	TP	1	0.999 (1)	TP
Lumbar/ Thoracic Spine	0	0.493 (0)	TN	0	0.9 (1)	FP	0	0.155 (0)	TN
Shoulder	0	N/A	---	0	N/A	---	0	N/A	---
Arm	0	N/A	---	1	N/A	---	0	N/A	---
Forearm	0	N/A	---	0	N/A	---	0	N/A	---
Pelvis	0	N/A	---	0	N/A	---	0	N/A	---
Thigh	1	0.334 (0)	FN	0	0.007 (0)	TN	0	0.005 (0)	TN
Knee	0	N/A	---	0	N/A	---	0	N/A	---
Leg	0	N/A	---	0	N/A	---	0	N/A	---
Ankle	0	N/A	---	0	N/A	---	0	N/A	---
Foot	0	N/A	---	0	N/A	---	0	N/A	---
		Accuracy : 80%			Accuracy : 80%			Accuracy : 100%	

VICIS Reconstruction – Vehicle Deformation

The comparison between real-world crash-deformed vehicles and their corresponding FE model simulations shows a strong similarity. As shown in Fig. 8, Fig. 9, the amount of bumper and hood deformation are well aligned between the reconstructed models and the observed crash vehicles. This indicates that the FE models effectively capture the structural response during pedestrian impacts.

Fig. 8. Visual comparison of vehicle deformation (front view).

Fig. 9. Visual comparison of vehicle deformation (top view).

VICIS Reconstruction vs. Component-Level Validation

This section explains the response of component-level test points in regions that were critical to the reconstruction cases. While Euro NCAP pedestrian impactor tests are conducted at approximately 25 mph, the reconstructed cases involved significantly higher impact speeds, making direct comparisons inappropriate. Moreover, there were no test points that exactly matched the conditions of the reconstruction cases. Given these limitations, relative trends were evaluated instead.

Only the upper and lower legform tests were included in the comparison. Headform tests were excluded because, in the Silverado and Rogue cases, substantial front-end and hood deformation occurred prior to head contact, making it difficult to align contact locations with those used in the undeformed test conditions. Additionally, none of the headform test points closely corresponded to the contact location observed in the Camry case. Therefore, only upper and lower legform data were used for this comparison.

The impactor test locations most closely matched to the real-world pedestrian contact points were: UL1652 and LL1616 for the Silverado; UL1611 and LL1611 for the Rogue; and U-7 and L-7 for the Camry (Appendix A). Injury trends from the component tests for upper and lower legform impacts, aligned with femur and tibia injury outcomes observed in the reconstructions. In the reconstruction simulations, the Silverado showed a relatively high probability of AIS 3+ thigh injury (over 30%) and AIS 2+ leg injury (over 50%), while both the Camry and Rogue predicted near-zero probabilities for AIS 3+ thigh injuries and around 10% for AIS 2+ leg injuries. These results were consistent with real-world observations and component-level test data. Only the Silverado case showed observed thigh and leg injuries and exceeded upper bound of threshold values in both upper and lower legform tests, resulting in a score of zero for pedestrian protection. This consistency suggests that component-validation tests can reflect the influence of front-end design on pedestrian injury risk.

IV. DISCUSSION

Pedestrian kinematics varied depending on vehicle type, aligning well with previously reported trends. For example, in the Camry case, representing sedans, the THUMS model showed initial contact at the lower extremities with the bumper, followed by pelvis contact, torso rotation, and sliding up the hood before head strike. In contrast, the Rogue case, representing SUVs, exhibited more direct engagement of the femur and pelvis with the vehicle front-end. The legs remained pinned under the bumper at the time of head impact, restricting torso sliding and resulting in a higher center of rotation. These kinematic responses are consistent with findings from prior full-scale pedestrian impact tests with PMHS [22] and HBM simulations [23]. Importantly, this study also included a pickup truck case (Silverado), whereas few prior studies have investigated pedestrian kinematics in truck collisions using HBMs. The current simulation of the Silverado case revealed no evidence of torso sliding, indicating that the thorax was directly engaged by the HLE early in the impact, resulting in limited upper body rotation and more localized thoracic loading. This pattern aligns with recent field data findings showing that trucks pose a unique threat to pedestrian safety, particularly in thoracic injuries in the U.S. [15-16].

In the component validation, the upper legform test conditions showed notable discrepancies, whereas the other cases generally aligned well with the test data. The Camry model exhibited expected differences, given its dimensional and geometric differences from the tested A4 and Malibu sedans. Among the models, the Rogue was expected to show the most similar response in upper legform test conditions due to its closely matching front-end geometry to the tested vehicle. It was true that the Rogue showed similar force and moment responses, although some discrepancies were observed in velocity deceleration. One potential explanation for this is the simplified boundary conditions used in the simulation. While the experimental test utilized a linear guide structure to control upper legform motion, the simulation allowed motion in only one vector direction through constraints applied to a rigid part. This likely led to greater rebound than in the experimental test, due to the absence of structural support, friction, and damping effects. However, this discrepancy likely had a minor effect on injury prediction, as the loading phase was similar, resulting in similar force and moment responses. In contrast, the Silverado model showed higher initial deceleration and greater lower femur force values compared to the test. Fig. 10 compares a single test condition between the Tahoe and Silverado. The upper legform includes a 675 Nm torque limiting joint, which begins to rotate once the threshold is exceeded. At 15 ms, the Silverado shows greater rotation than the Tahoe, and by 20 ms, the Tahoe no longer shows rotation increase while the Silverado continues to rotate further. This suggests that greater force was applied to the lower part of the upper legform in the Silverado case. Although the Silverado shares a platform with the Tahoe, its front bumper and grille transition zone has a more squared geometry, meaning the bumper protrudes further relative to the grille, creating a more aggressive front-end contour unlike the rounded shape of the Tahoe (Fig. 10). Both stiffness and bumper geometry appear to contribute to force concentration in the lower femur region.

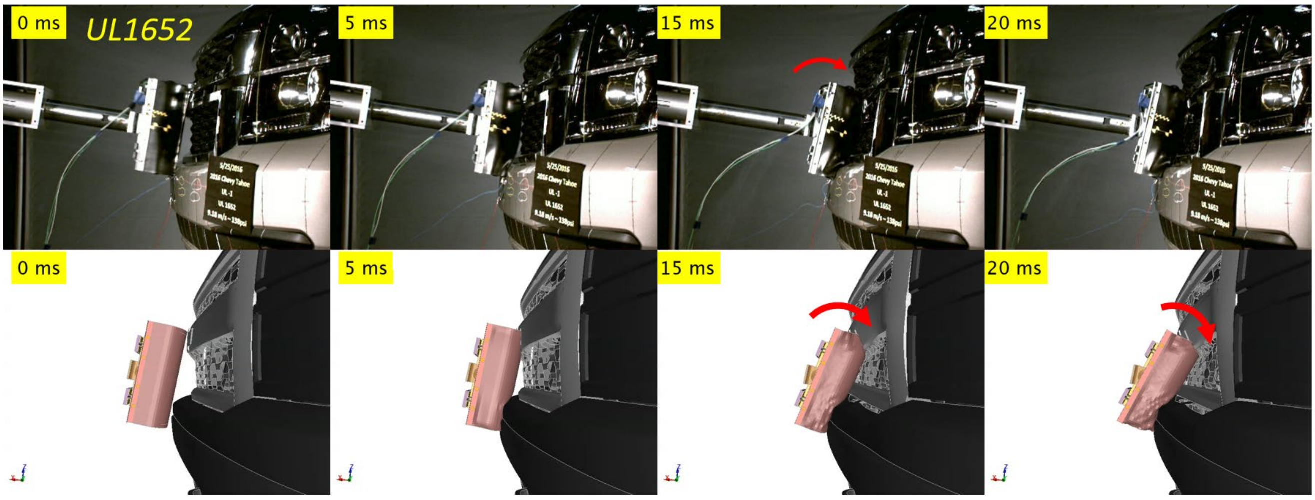

Fig. 10. Comparison of Upper legform impact (top: 2016 Chevrolet Tahoe, bottom: 2014 Chevrolet Silverado).

One finding was that injury trends predicted by Euro NCAP component tests, particularly for upper and lower legform impacts, aligned with real-world femur and tibia injury patterns observed in the VICIS cases. In the reconstruction, the Silverado case exhibited notably higher injury probabilities in the thigh and leg regions compared to the other cases, despite having an impact speed (45 mph) that fell between that of the Camry (37 mph) and the Rogue (55 mph). While the actual impact speed for the Silverado was unknown and the speed limit (45 mph) was used as an estimate, the injury prediction trend still appeared consistent in the simulation results. For AIS 3+ thigh injuries, Silverado showed over a 30% chance of injury, whereas other cases predicted near-zero probabilities. This outcome aligns with component test results for the upper legform, where only the Silverado's data exceeded the Euro NCAP evaluation threshold. These findings suggest that Silverado’s front-end structure, specifically the bumper and grille transition zone, may contribute disproportionately to pedestrian injuries. In terms of leg injuries, a similar pattern was observed. Silverado showed a 50% likelihood of AIS 2+ leg injuries in the simulation, while the Camry and Rogue exhibited approximately 10% probabilities, closely matching the real-world VICIS data. Component test results supported this trend as well, as the Silverado's lower legform tests indicated that both the tibia upper bending moment and Knee MCL exceeded the injury thresholds. These consistent results across component testing and reconstructions suggest that component tests can capture the influence of front-end geometry on pedestrian injury outcomes. However, while the established pedestrian crashworthiness standards may be applicable for evaluating leg injuries caused by bumper impacts in trucks, there remains an untested region in the hood to grille transition zone of larger and taller vehicles that may require additional consideration.

Across all reconstruction cases, thoracic injuries were consistently predicted to be severe. In particular, the Rogue and Silverado cases showed high strain values in the lower ribs (ribs 8–12), as illustrated in Fig. 11. Existing pedestrian safety protocols, such as the Euro NCAP procedures, do not account for thoracic impacts from higher-profile, flat, or box-shaped vehicle fronts, including SUVs, trucks, and vans. It is evident that this untested region plays a significant role in thoracic loading, as supported by previous simulation studies [23–25], field data analyses [15–16], and the findings of this study.

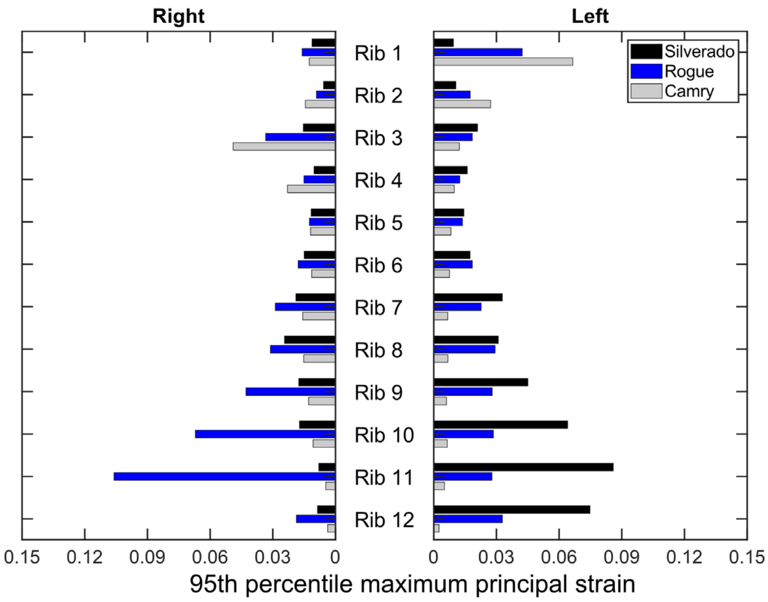

Fig. 11. Rib strain distributions across vehicle types.

As thoracic injuries often involve complex rib fracture mechanisms that are highly sensitive to impact location and cannot be sufficiently captured by conventional deflection-based metrics, advanced modeling techniques are essential. Previous studies have proposed thorax-specific evaluation approaches using Thorax Injury Prediction Tool (TIPT) [26] and WordSID thorax module [27]. However, these tools are limited in replicating the complex oblique (rather than perpendicular) loading experienced during real-world impacts. In fact, the locations of maximum rib deflection and maximum rib strain were found to differ, and the WordSID thorax module also face limitations in replicating human spine bending [27]. These findings underscore the need for injury assessment approaches that can evaluate deformation or strain across several rib locations simultaneously. The development of physical dummies with improved thorax biofidelity may produce viable approach, however, such efforts require significant time and resources. On the other hand, virtual evaluations using high-fidelity FE HBMs offer a promising alternative. As shown by [28], strain-based rib fracture prediction methods can be integrated into evaluation protocols to assess thoracic injury risks more accurately. These virtual tools allow for detailed, multi-point strain assessments that better reflect real-world injury mechanisms and could fill the current gap in evaluating impacts to untested regions like the HLE.

This study has several limitations. First, all reconstruction cases involved high-impact speeds, with every scenario exceeding 35 mph, typically associated with fatality-level injuries [4]. While NHTSA suggests 25 mph testing as a standard benchmark for pedestrian safety evaluation, the selected cases reflect more severe real-world collisions. As a result, the simulations may not effectively distinguish injury mechanisms specific to different vehicle types under lower-speed conditions. Second, due to insufficient data, the vehicle reconstructions required numerous assumptions in the presence of large and unaddressed uncertainties. For example, fairly small posture and anthropometric characteristics can influence injury outcomes. However, only a single posture was investigated for each case, so the sensitivity of the outcomes to these and other unexplored variables such as pedestrian orientation, pedestrian movement, and vehicle braking is unknown. Third, there are limitations in making a detailed comparison between injury outcomes predicted by the HBM and those reported in the VICIS data. As a result, we relied on the MAIS values reported for specific body regions in the VICIS database, even though the injury prediction suite is capable of identifying fractures in specific bones (e.g., femur and tibia). Lastly, as shown in Table I, the simulation vehicle models are not identical to those used in the component tests and the VICIS cases, which may contribute to discrepancies in impactor responses and injury outcomes. Nevertheless, results from component-level validation and comparisons with real-world AIS 2+ and AIS 3+ injury data suggest that impactor responses and pedestrian injury predictions are more sensitive to variations in vehicle front-end geometry.

V. CONCLUSION

This study reconstructed three real-world pedestrian crash cases to investigate injury variability across the diverse U.S. vehicle fleet using deformable FE vehicle models representing trucks, SUVs, and sedans. The applicability of current pedestrian safety testing protocols was also checked by comparing crash reconstruction results with Euro NCAP-style impactor responses. While the impactor responses, particularly in the upper and lower leg regions, aligned with both simulation results and real-world injury outcomes, severe thoracic loading in larger and taller vehicles occurred in untested areas under current protocols. These results highlight the limitation of applying existing pedestrian safety standards to the U.S. vehicle fleet, which is dominated by SUVs and trucks. This study underscores the need to revise current regulations to include vehicle-specific safety evaluations that account for variations in size, geometry, and structural stiffness. Although the simulation vehicles were not identical to those used in the component tests and real-world crashes, the simulation results captured the influence of front-end geometry, which appears to be a primary factor in pedestrian injury outcomes. Furthermore, the alignment between impactor responses and real-world injury outcomes, along with the results of component-level validation, supports the use of deformable FE vehicle models to improve impactor-based test protocols and enable large-scale parametric studies for pedestrian safety assessment.

VI. ACKNOWLEDGEMENTS

The author gratefully acknowledges the NHTSA for sponsoring this research and providing insightful feedback that supported the development and validation of the simulations presented in this study.

VII. REFERENCES

[1] Schneider, R. J. (2020). United States pedestrian fatality trends, 1977 to 2016. Transportation research record, 2674(9), 1069-1083.

[2] Hu, W., & Cicchino, J. B. (2018). An examination of the increases in pedestrian motor-vehicle crash fatalities during 2009–2016. Journal of safety research, 67, 37-44.

[3] Sanchez Rodriguez, O., & Ferenchak, N. N. (2024). Longitudinal spatial trends in US pedestrian fatalities, 1999–2020. Transportation research record, 2678(5), 904-916.

[4] NHTSA, 88 FR 34366 - New Car Assessment Program, Request for comments (RFC). Federal Register Volume 88, Issue 102 (May 26, 2023).

[5] European New Car Assessment Programme (Euro NCAP). (2017) Assessment Protocol – Pedestrian Protection, Version 9.0.2, pp.1–18. Euro NCAP, Brussels.

[6] United Nations Economic Commission for Europe (UNECE). (2009) Global Technical Regulation No. 9:

Pedestrian Safety. ECE/TRANS/180/Add.9, United Nations, Geneva.

[7] European Experimental Vehicles Committee, 1994. “EEVC Working Group 10 report. Proposals for methods to evaluate pedestrian protection.”

[8] European Enhanced Vehicle-safety Committee. "EEVC Working Group 17 Report—Improved Test Methods to Evaluate Pedestrian Protection Afforded by Passenger Cars." TN0 Crash-Safety Research Centre: Delft, The Netherlands (1998): 6-8.

[9] The European Automobile Manufacturers’ Association, (ACEA) "New passenger cars by segment in the EU" 18 May 2023. https://www.acea.auto/figure/new-passenger-cars-by-segment-in-eu/

[10] New York Times, "Rise of S.U.V.s: Leaving Cars in Their Dust, With No Signs of Slowing" May 21, 2020, https://www.nytimes.com/2020/05/21/business/suv-sales-best-sellers.html

[11] Desapriya, E., Subzwari, S., Sasges, D., Basic, A., Alidina, A., Turcotte, K., & Pike, I. (2010). Do light truck vehicles (LTV) impose greater risk of pedestrian injury than passenger cars? A meta-analysis and systematic review. Traffic injury prevention, 11(1), 48-56.

[12] Edwards, M., & Leonard, D. (2022). Effects of large vehicles on pedestrian and pedalcyclist injury severity. Journal of safety research, 82, 275-282.

[13] Mallory, A., Ramachandra, R., Valek, A., Suntay, B., & Stammen, J. (2024). Pedestrian injuries in the United States: shifting injury patterns with the introduction of pedestrian protection into the passenger vehicle fleet. Traffic injury prevention, 25(3), 463-471.

[14] Monfort, S. S., & Mueller, B. C. (2020). Pedestrian injuries from cars and SUVs: Updated crash outcomes from the vulnerable road user injury prevention alliance (VIPA). Traffic injury prevention, 21(sup1), S165-S167.

[15] Mueller, B. C., Monfort, S. S., & Jermakian, J. S. (2024). Role of pedestrian waist and hip height relative to the vehicle front end in kinematics and torso injuries.

[16] Monfort, S. S., Hu, W., & Mueller, B. C. (2024). Vehicle front-end geometry and in-depth pedestrian injury outcomes. Traffic injury prevention, 25(4), 631-639.

[17] Schubert, A., Babisch, S., Scanlon, J. M., Campolettano, E. T., Roessler, R., Unger, T., & McMurry, T. L. (2023). Passenger and heavy vehicle collisions with pedestrians: assessment of injury mechanisms and risk. Accident Analysis & Prevention, 190, 107139.

[18] Hu, J., Flannagan, C., Ganesan, S., Bowman, P., Sun, W., Farooq, I., ... & Rupp, J. (2023). Understanding the new trends in pedestrian injury distribution and mechanism through data linkage and modeling. Accident Analysis & Prevention, 188, 107095.

[19] Lalwala, M., Chawla, A., Thomas, P., & Mukherjee, S. (2020). Finite element reconstruction of real-world pedestrian accidents using THUMS pedestrian model. International journal of crashworthiness.

[20] https://www.ccsa.gmu.edu/models/

[21] Suntay, B., Stammen, J., & Martin, P. (2019). Pedestrian Protection–Assessment of the US Vehicle Fleet (No. DOT HS 812 723). United States. Department of Transportation. National Highway Traffic Safety Administration.

[22] Kerrigan, J., Kam, C., Drinkwater, C., Murphy, D., Bose, D., Ivarsson, J., & Crandall, J. (2005). Kinematic comparison of the Polar-II and PMHS in pedestrian impact tests with a sport-utility vehicle. Proceedings of the 2005 International Research Council on the Biomechanics of Impact (IRCOBI), Prague, Czech Republic.

[23] Han, Y., Yang, J., Nishimoto, K., Mizuno, K., Matsui, Y., Nakane, D., ... & Hitosugi, M. (2012). Finite element analysis of kinematic behaviour and injuries to pedestrians in vehicle collisions. *International Journal of Crashworthiness*, *17*(2), 141-152.

[24] Li, G., Nie, J., Yang, J., Zhou, X., Zhang, C., Yu, X., ... & Wang, M. (2013). A study on injuries and kinematics in pedestrian accidents involved minivan and sedan.

[25] Wang, F., Yu, C., Li, G., Han, Y., Wang, B., Yang, J., & Lan, D. (2018). A Study on Influence of Minivan Front-End Design and Impact Velocity on Pedestrian Thorax Kinematics and Injury Risk. *Applied bionics and biomechanics*, *2018*(1), 7350159.

[26] Zander, O., Wisch, M., Ott, J., Burleigh, M., Fornells, A., & Lundgren, C. (2019). Development and evaluation of a thorax injury prediction tool (TIPT) and possibilities for incorporation within improved test and assessment procedures–results from SENIORS.

[27]Chang, Y., Long, Y., Wan, X., Liu, Y., Wang, G., Zhang, G., & Xiao, Z. (2024). A study on the performance of WordSID thorax module for thorax injury prediction in e-Bike rider based on real accident data. *Acta of Bioengineering & Biomechanics*, *26*(3).

[28]Forman, J., Kulkarni, S., Perez-Rapela, D., Mukherjee, S., Panzer, M., & Hallman, J. (2022, June). A method for thoracic injury risk function development for human body models. In *IRCOBI Conference. Porto, Portugal* (pp. 12-15).

[29]Frazier, H., & Flanders, A. R. (2025). Review of Literature Addressing Effects of Pedestrian Safety-Related Test Requirements on Vehicle Design, Fleet Composition, and Pedestrian Injury—Task 2.

[30]McQuistion, I., & Flanders, A. R. (2025). Review of Literature Addressing Vehicle Pedestrian Safety Market Trends—Task 3.

[31]ISO/TS 18571:2024 Road Vehicles — Objective Rating Metric for Non-ambiguous Signals, 2024.

[32]Eppinger, R., Kuppa, S., Saul, R., & Sun, E. (2000). Supplement: development of improved injury criteria for the assessment of advanced automotive restraint systems: Ii.

[33]ROSSI, M. (2020). Assessment of a numerical procedure to evaluate the safety performance of an FHR device in terms of human neck loads.

[34]Forman, J., Kulkarni, S., Perez-Rapela, D., Mukherjee, S., Panzer, M., & Hallman, J. (2022, June). A method for thoracic injury risk function development for human body models. In *IRCOBI Conference. Porto, Portugal* (pp. 12-15).

[35]Tushak, S. K., Gepner, B. D., Forman, J. L., Hallman, J. J., Pipkorn, B., & Kerrigan, J. R. (2023). Human lumbar spine injury risk in dynamic combined compression and flexion loading. *Annals of biomedical engineering*, *51*(6), 1216-1225.

[36]Santago, A. C., Cormier, J. M., & Duma, S. M. (2008). Humerus fracture bending risk function for the 50th percentile male. *Biomedical sciences instrumentation*, *44*, 231-236.

[37]Santago, Anthony C., et al. "Forearm fracture bending risk functin for the 50th percentile male." *Biomedical sciences instrumentation* 44 (2008): 201-206.

[38]Gunji, Y., Okamoto, M., & Takahashi, Y. (2012, September). Examination of human body mass influence on pedestrian pelvis injury prediction using a human FE model. In *Proceedings of the International Research Council on the Biomechanics of Injury conference* (Vol. 40, pp. 316-327). International Research Council on Biomechanics of Injury.

[39]Kerrigan, J. R., Drinkwater, D. C., Kam, C. Y., Murphy, D. B., Ivarsson, B. J., Crandall, J. R., & Patrie, J. (2004). Tolerance of the human leg and thigh in dynamic latero-medial bending. *International Journal of Crashworthiness*, *9*(6), 607-623.

[40]Mo, F., Arnoux, P. J., Cesari, D., & Masson, C. (2014). Investigation of the injury threshold of knee ligaments by the parametric study of car–pedestrian impact conditions. *Safety science*, *62*, 58-67.

[41]Kuppa, S., Wang, J., Haffner, M., & Eppinger, R. (2001). *Lower extremity injuries and associated injury criteria* (No. 2001-06-0160). SAE Technical Paper.

[42]Kulkarni, A., Chong, D., & Batarseh, F. A. (2020). Foundations of data imbalance and solutions for a data democracy. In Data democracy (pp. 83-106). Academic Press.

[43]Lockerby, J. W., Rudd, R. W., Martin, P. G., Rupp, J. D., Pintar, F. A., & Stitzel, J. D. Identifying Field Crash Data Collection Needs for a Pedestrian Crash Avoidance and Crashworthiness Study.

VIII. APPENDIX

Appendix A

Component Validation Results.

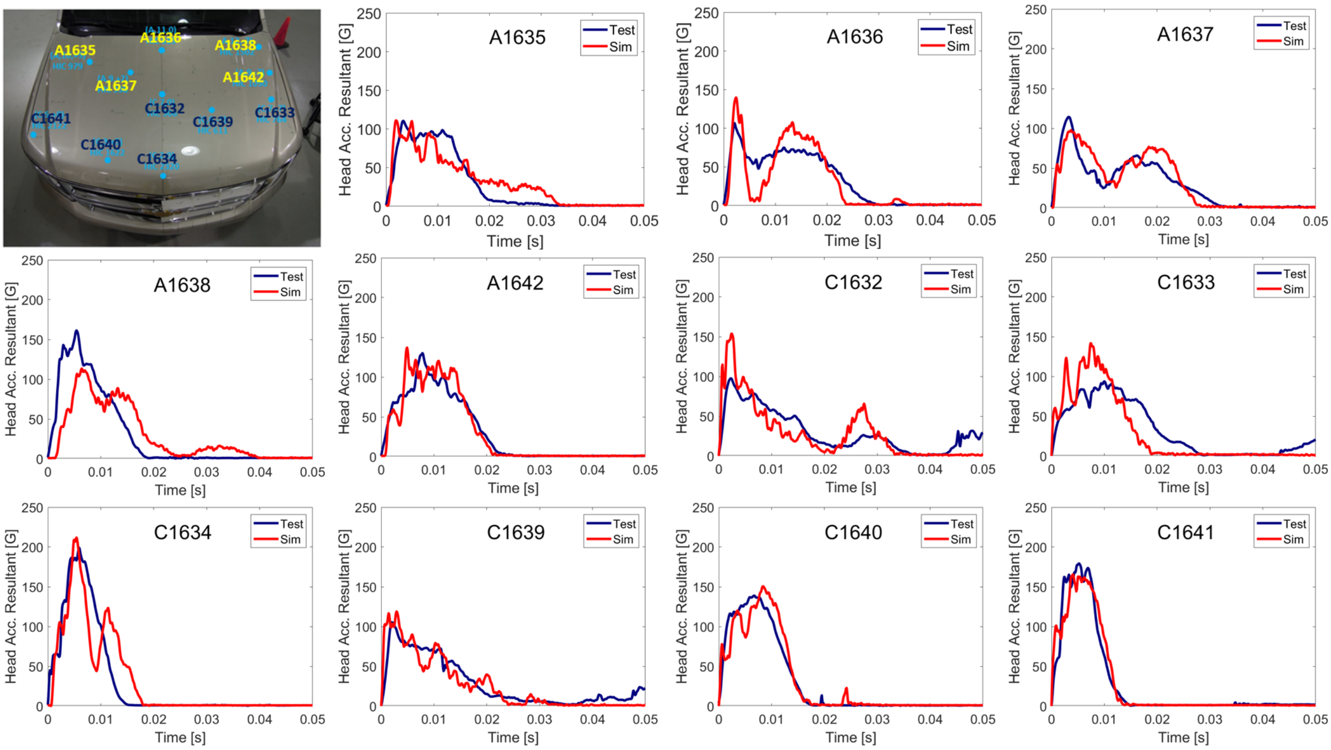

Fig. A1. Headform impactor responses: 2014 Chevrolet Silverado (Simulation).

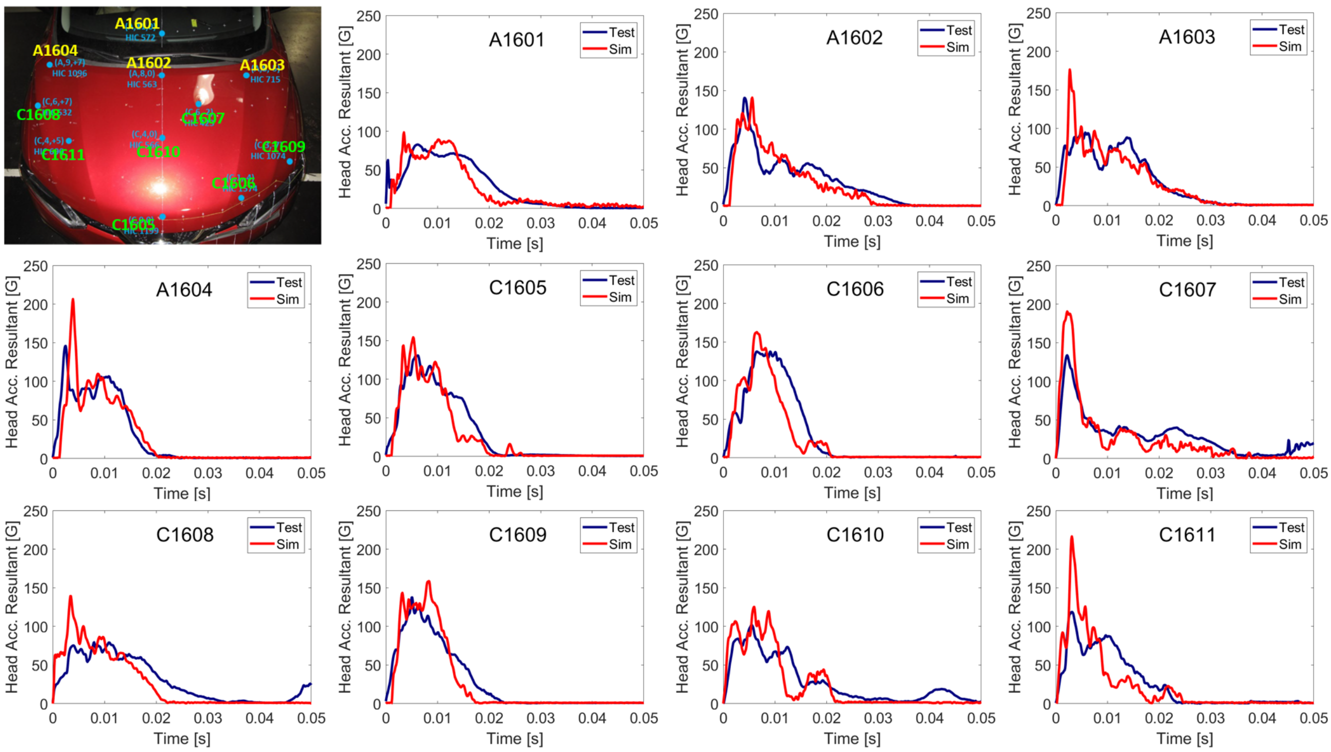

Fig. A2. Headform impactor responses: 2020 Nissan Rogue (Simulation).

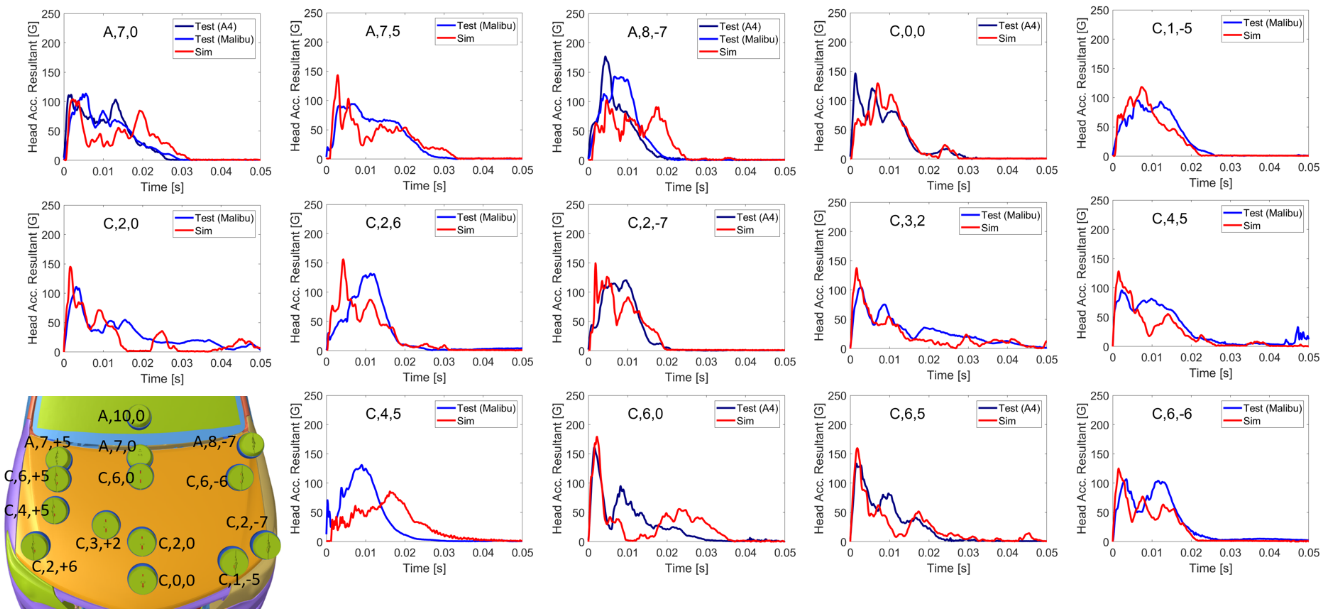

Fig. A3. Headform impactor responses: 2015 Toyota Camry (Simulation).

• UL1651

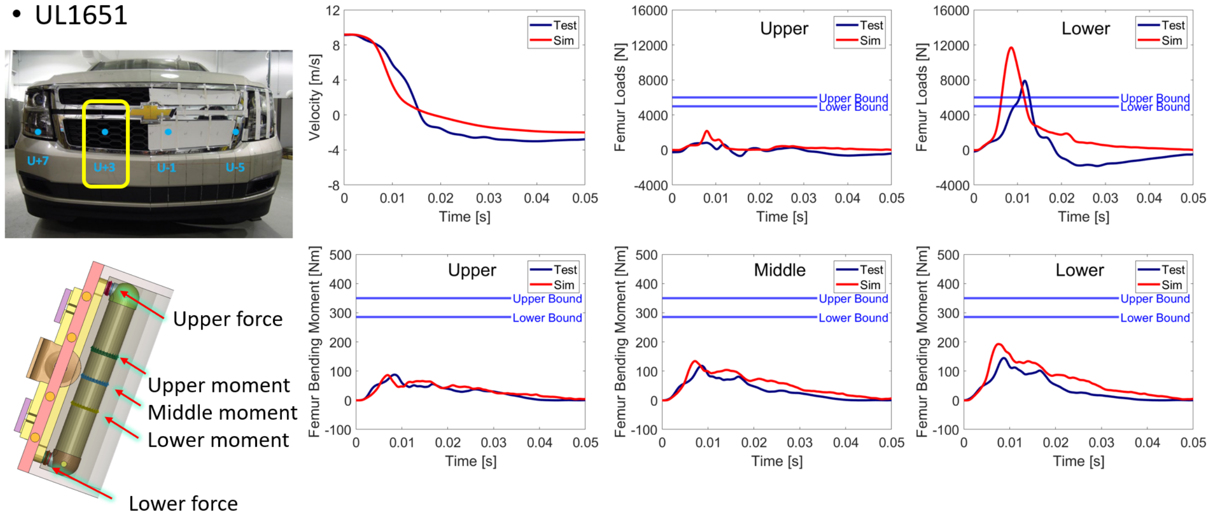

Fig. A4. Upper legform impactor responses: 2014 Chevrolet Silverado (Simulation).

• UL1652

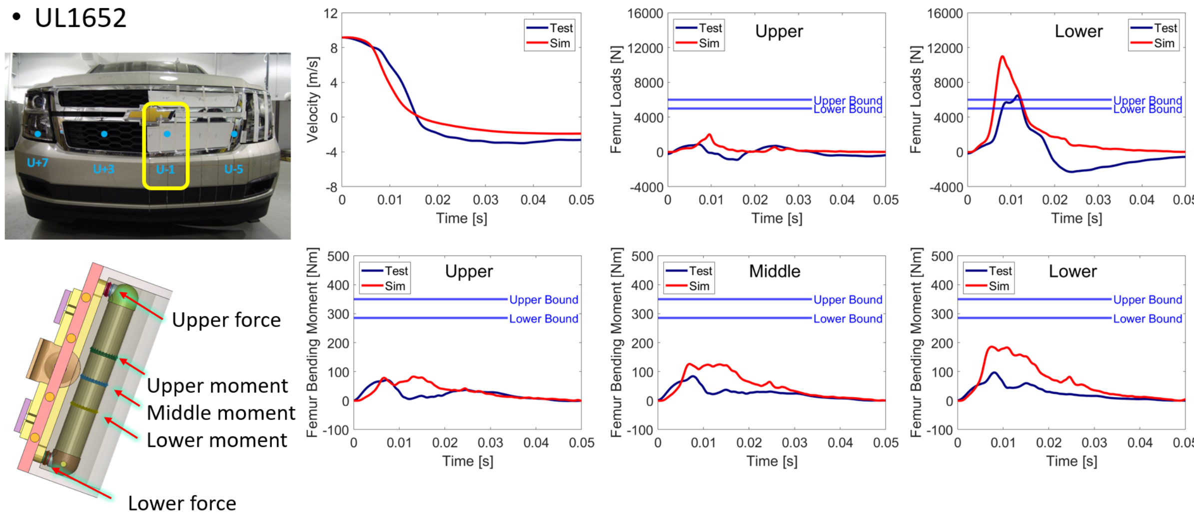

Fig. A5. Upper legform impactor responses: 2014 Chevrolet Silverado (Simulation).

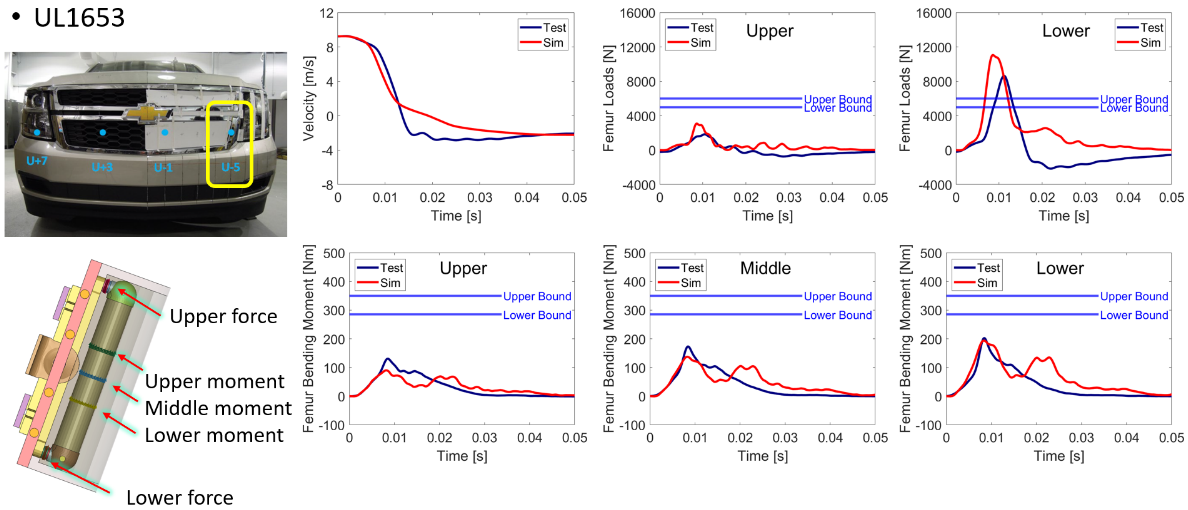

Fig. A6. Upper legform impactor responses: 2014 Chevrolet Silverado (Simulation).

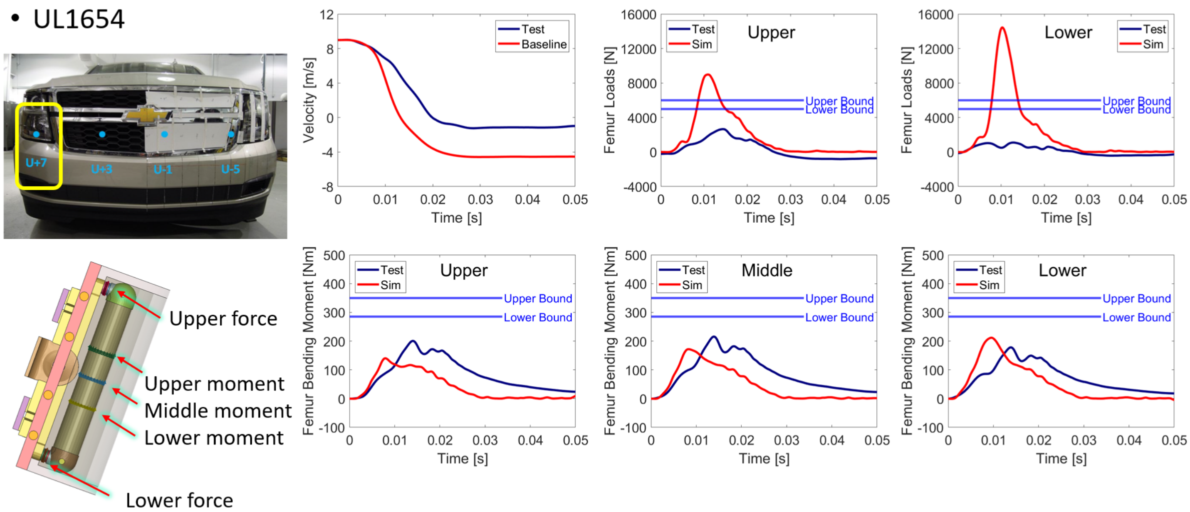

Fig. A7. Upper legform impactor responses: 2014 Chevrolet Silverado (Simulation).

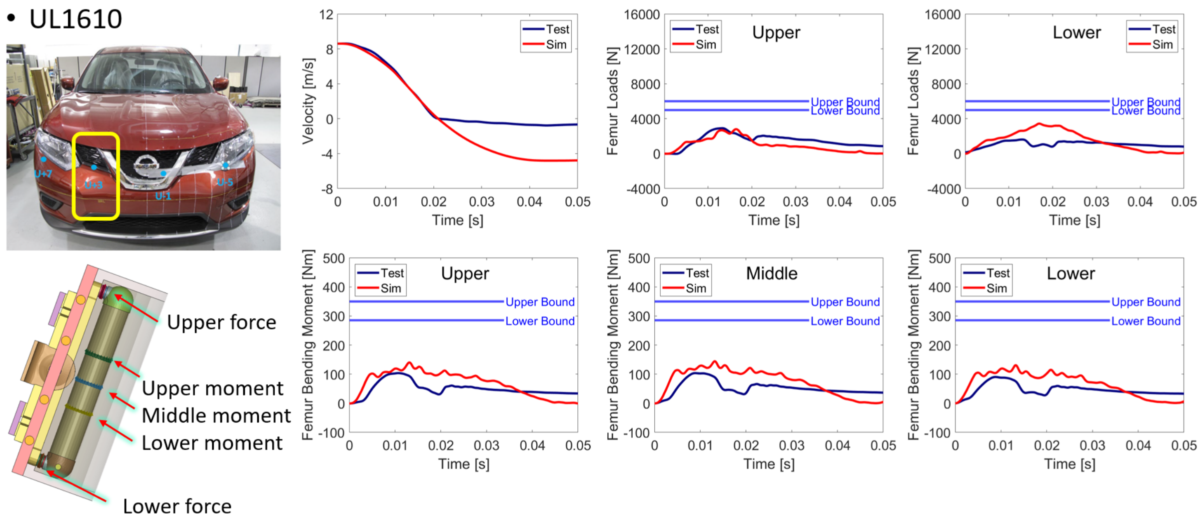

Fig. A8. Upper legform impactor responses: 2020 Nissan Rogue (Simulation).

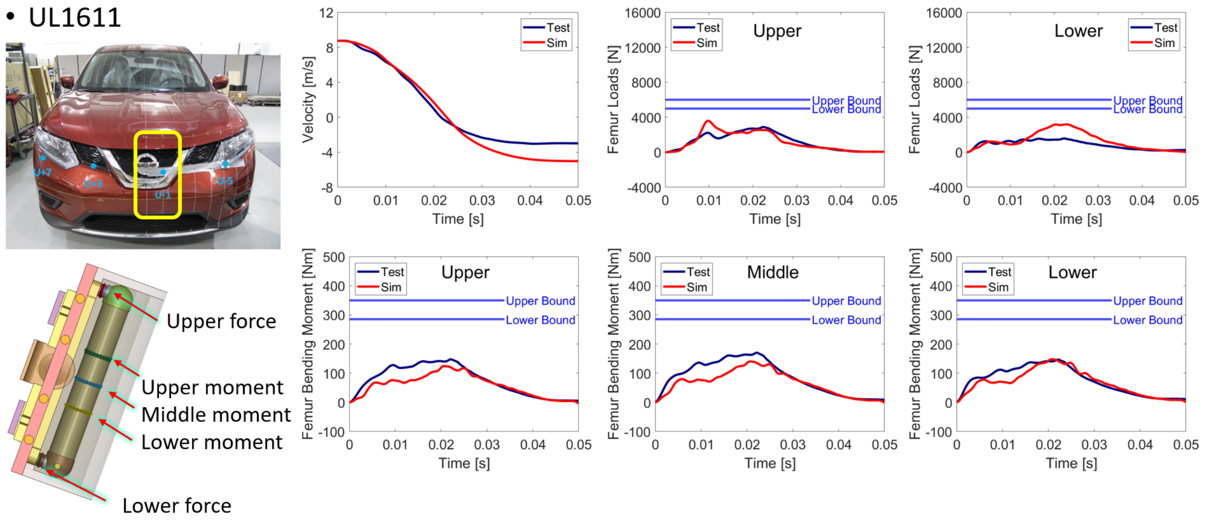

Fig. A9. Upper legform impactor responses: 2020 Nissan Rogue (Simulation).

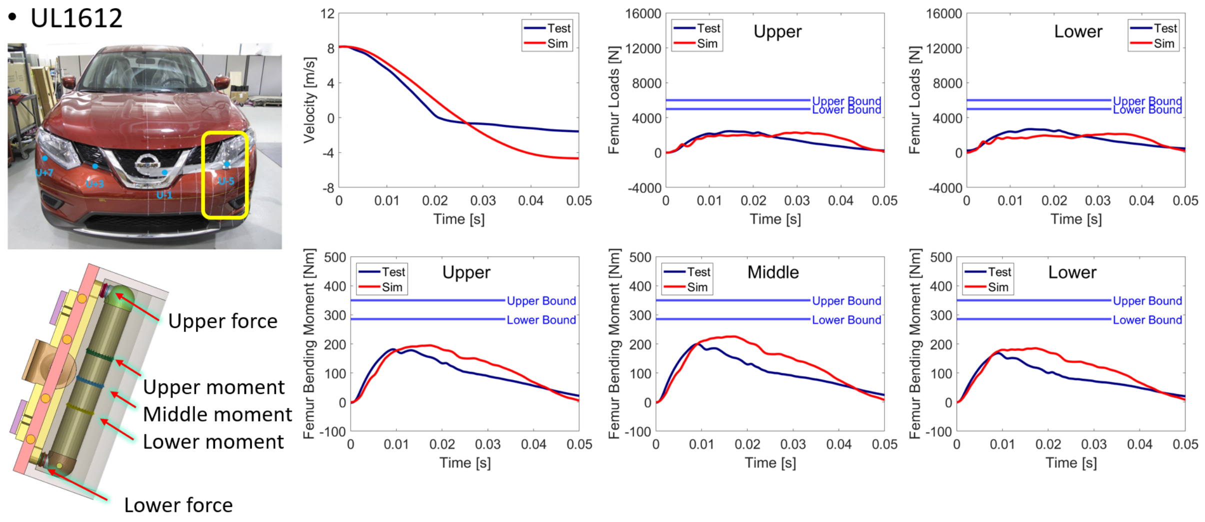

Fig. A10. Upper legform impactor responses: 2020 Nissan Rogue (Simulation).

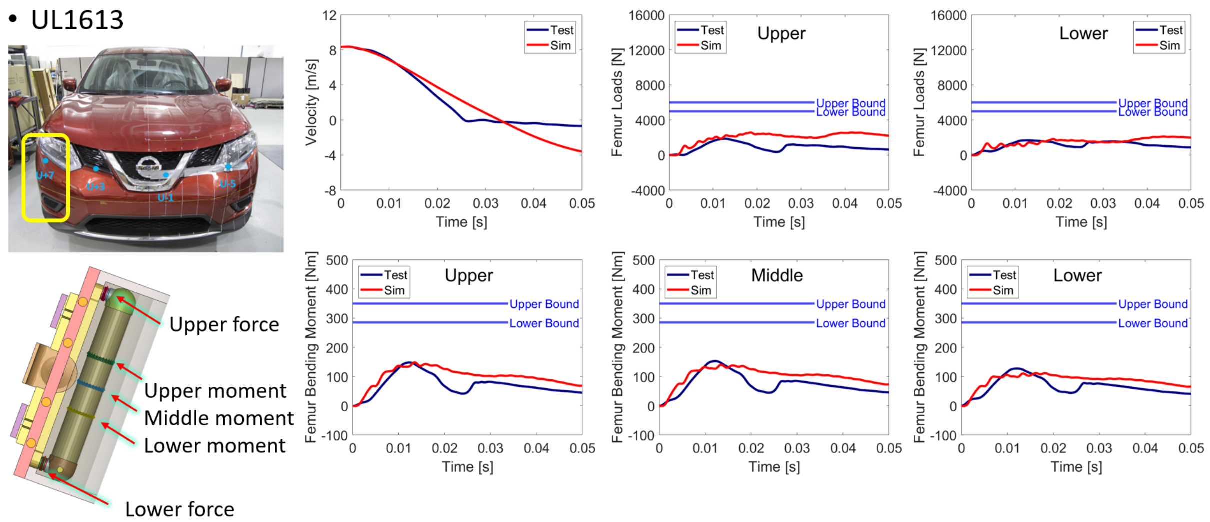

Fig. A11. Upper legform impactor responses: 2020 Nissan Rogue (Simulation).

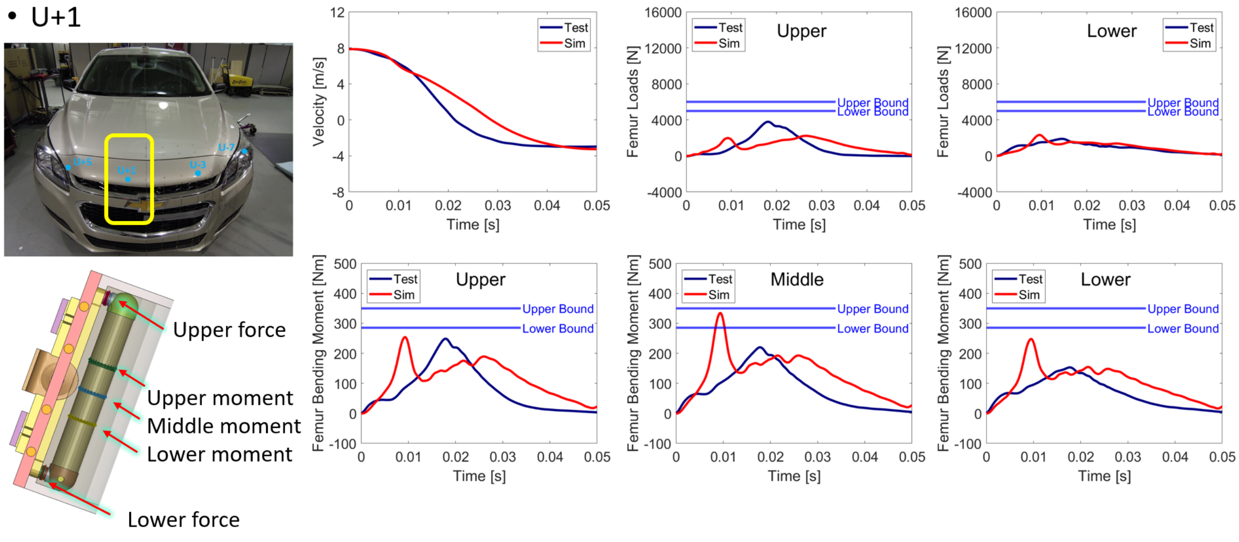

Fig. A12. Upper legform impactor responses: 2015 Toyota Camry (Simulation).

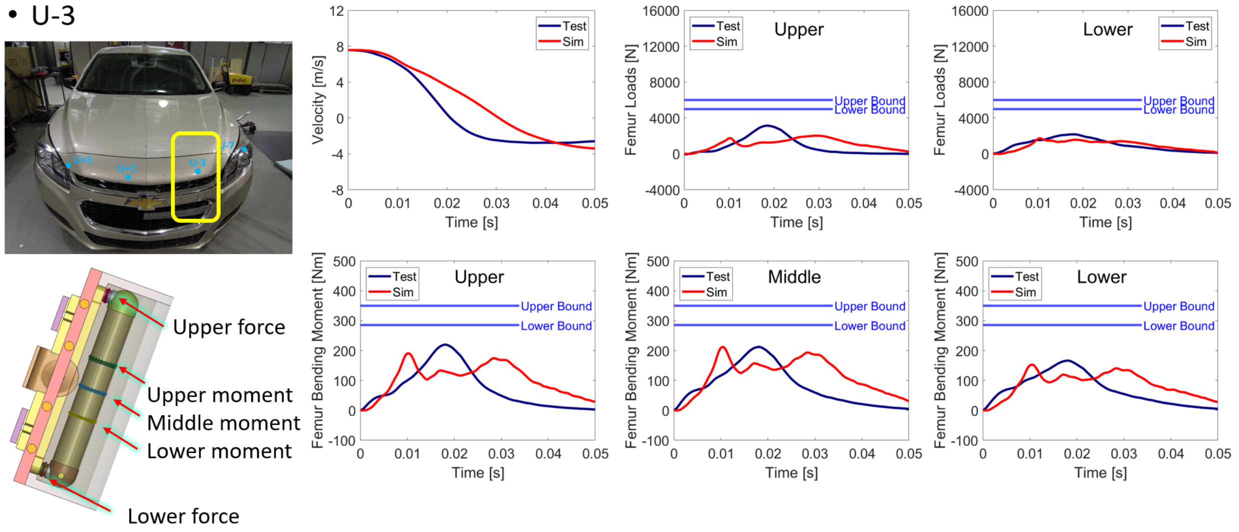

Fig. A13. Upper legform impactor responses: 2015 Toyota Camry (Simulation).

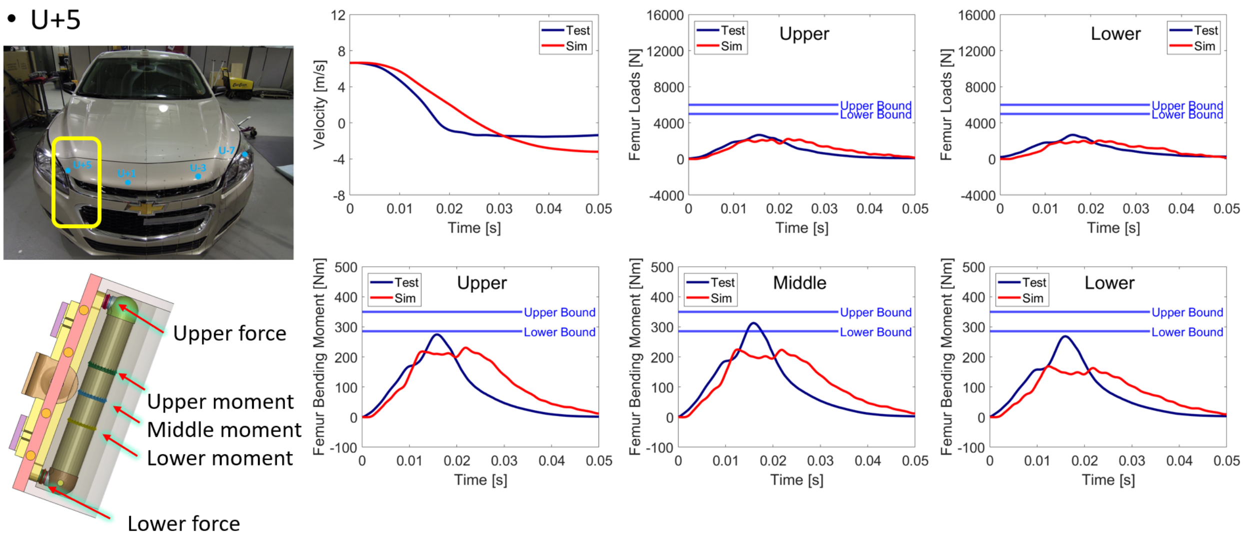

Fig. A14. Upper legform impactor responses: 2015 Toyota Camry (Simulation).

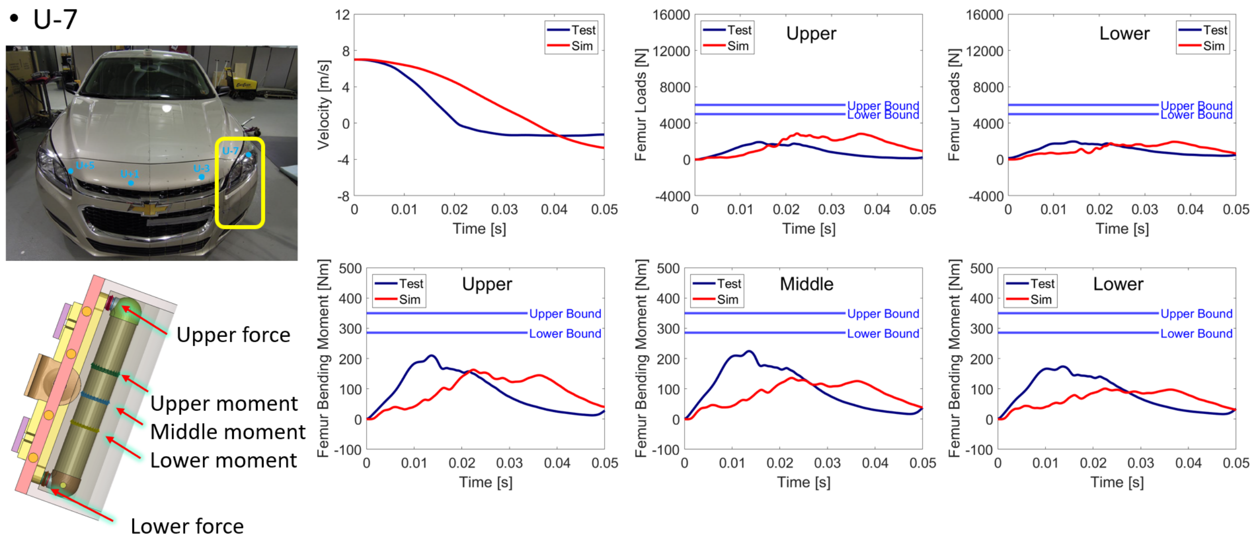

Fig. A15. Upper legform impactor responses: 2015 Toyota Camry (Simulation).

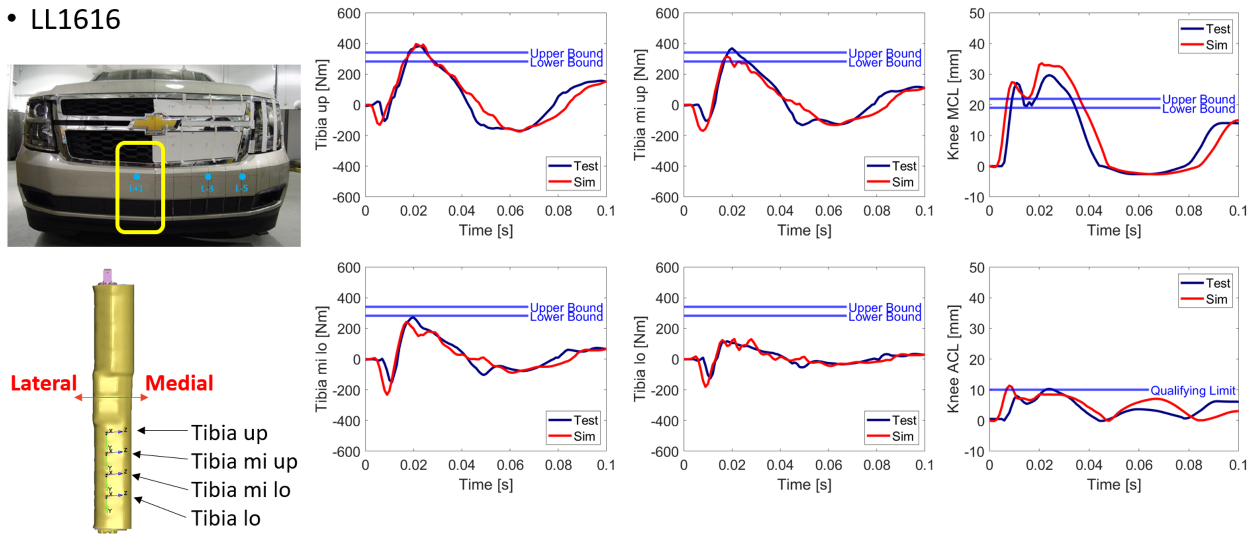

Fig. A16. Lower legform impactor responses: 2014 Chevrolet Silverado (Simulation).

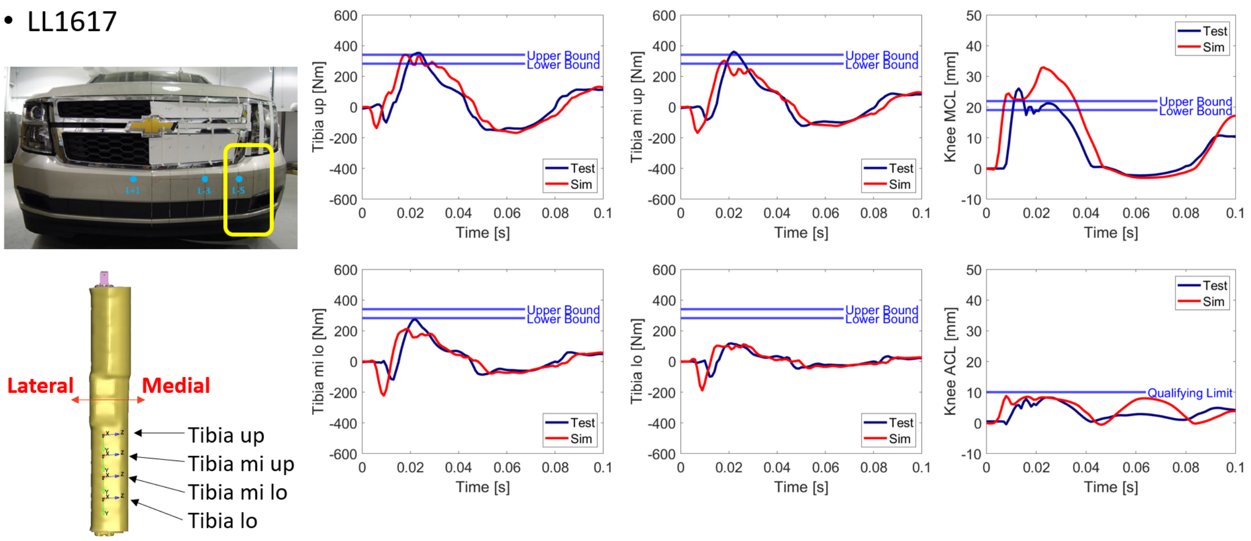

Fig. A17. Lower legform impactor responses: 2014 Chevrolet Silverado (Simulation).

- LL1618

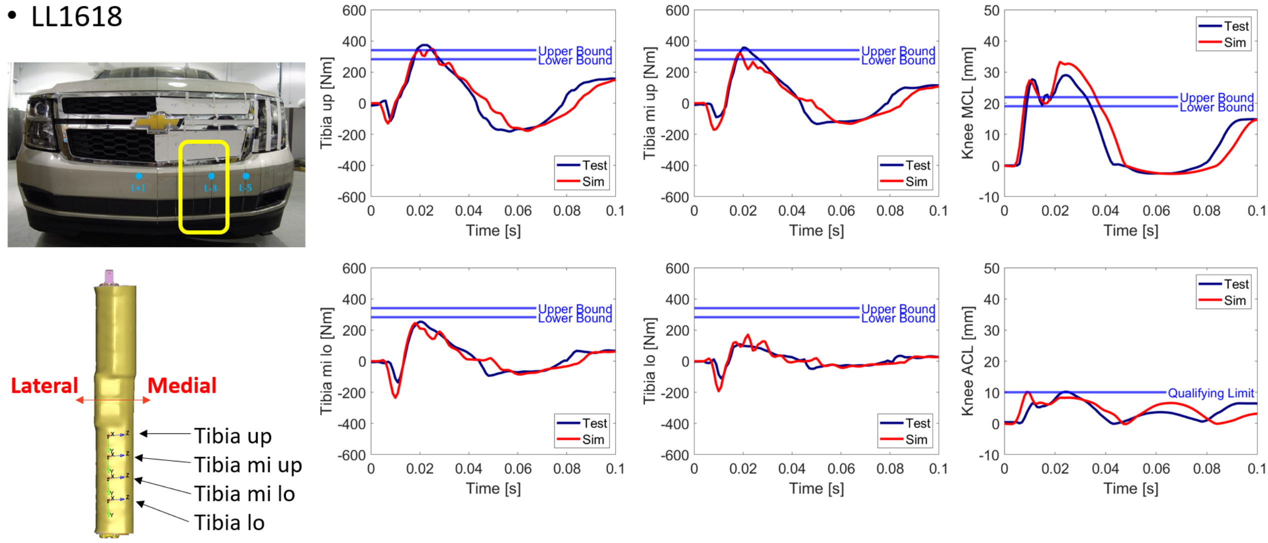

Fig. A18. Lower legform impactor responses: 2014 Chevrolet Silverado (Simulation).

- LL1605

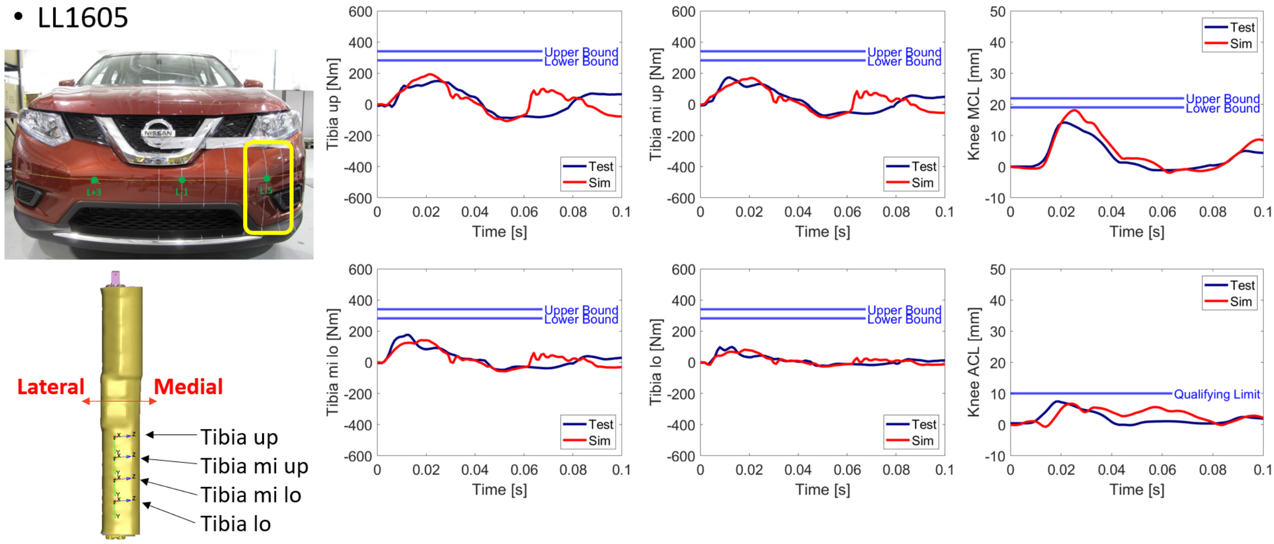

Fig. A19. Lower legform impactor responses: 2020 Nissan Rogue (Simulation).

- LL1606

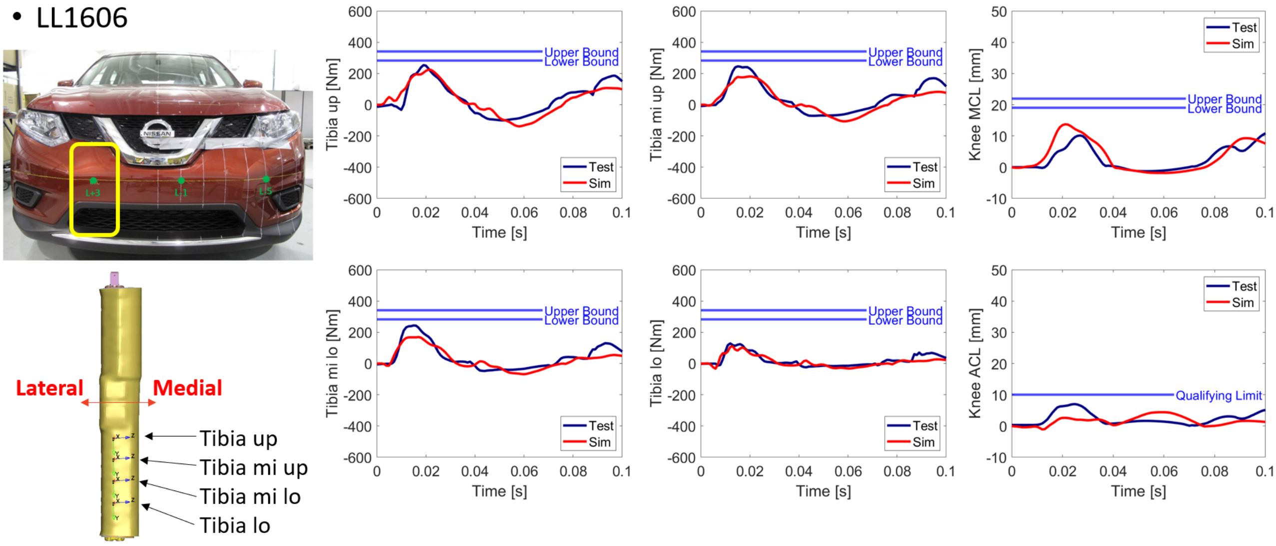

Fig. A20. Lower legform impactor responses: 2020 Nissan Rogue (Simulation).

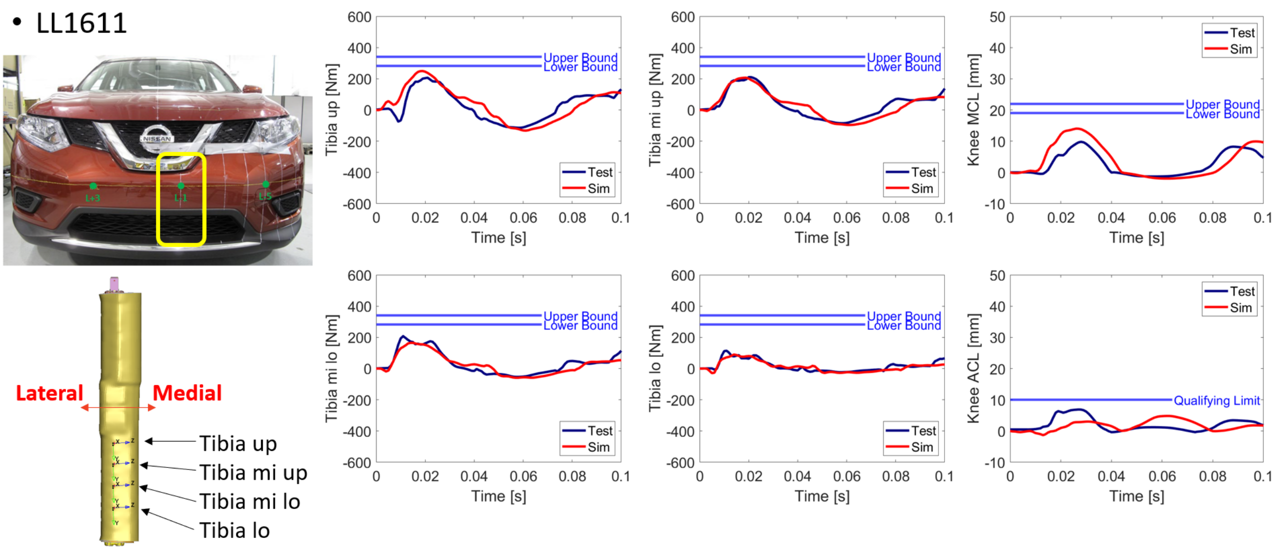

Fig. A21. Lower legform impactor responses: 2020 Nissan Rogue (Simulation).

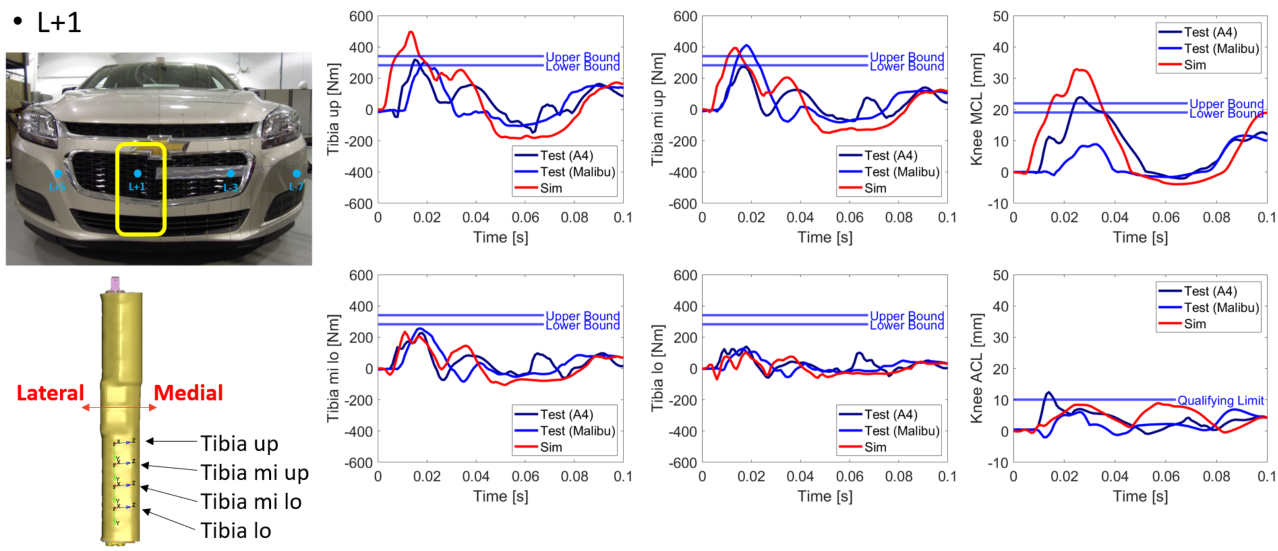

Fig. A22. Lower legform impactor responses: 2015 Toyota Camry (Simulation).

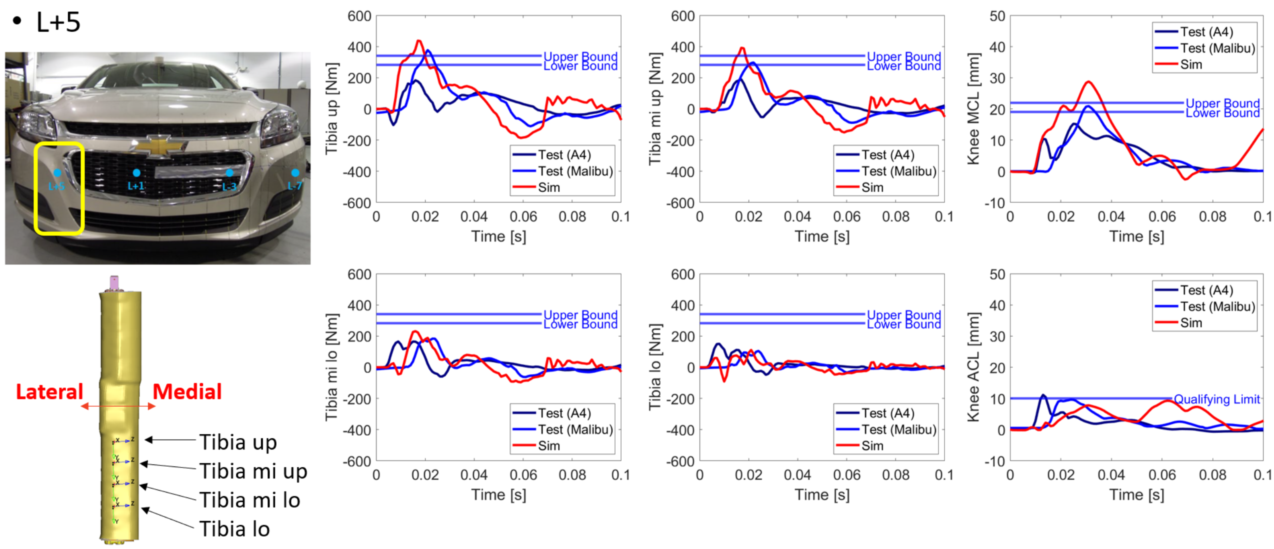

Fig. A23. Lower legform impactor responses: 2015 Toyota Camry (Simulation).

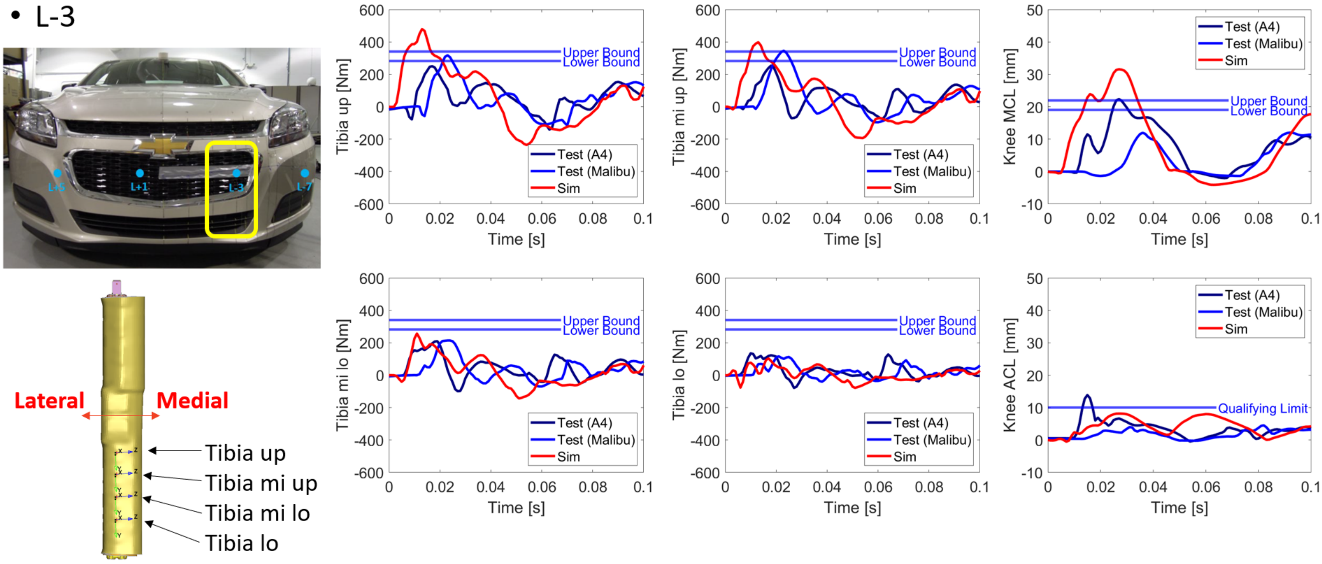

Fig. A24. Lower legform impactor responses: 2015 Toyota Camry (Simulation).

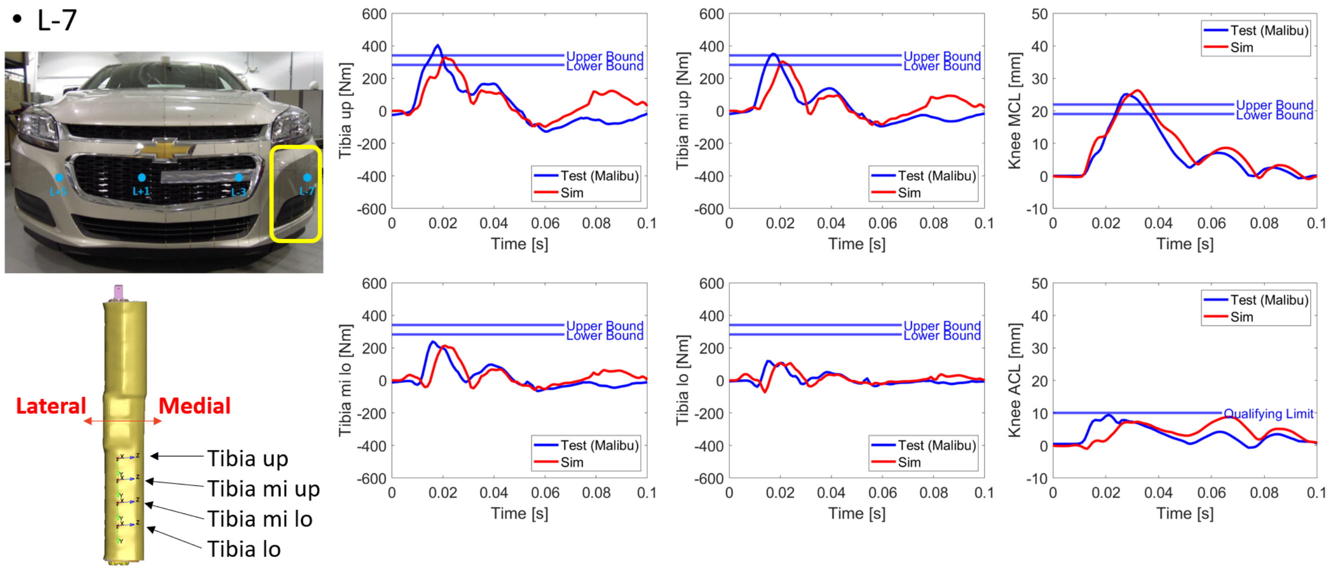

Fig. A25. Lower legform impactor responses: 2015 Toyota Camry (Simulation).